Programmed cell-immobilization of living cells by independent molecular interaction
(細胞膜へのクリック反応性官能基修飾の生細胞配置固定への応用)

２０２３

朱　程遠
ZHU CHENGYUAN

Contents

Preface

Programmed immobilization is markedly advancing the field of pharmaceutical research. This innovative methodology facilitates the manipulation of cells within controlled settings, such as multi-cell group co-cultures and three-dimensional tissue cultures. These advancements significantly enhance our understanding of complex biological processes, including drug metabolism, discovery, and tissue development. Such developments are not only instrumental in the enhancement of pharmaceutical efficacy but also lead the way for emerging therapeutic modalities, including personalized medicine and targeted drug delivery systems. Consequently, these advancements have profound implications for the future of medical treatment and intervention methodologies.

Cell immobilization techniques are generally classified into two categories: covalent binding and non-covalent binding. Covalent binding typically involves utilizing natural cell surface residues, such as thiol or amine ligands, for immobilization through chemical reactions. However, this method can interfere with the function of membrane proteins because it relies on natural amino acid residues in membrane proteins. Therefore, it is crucial to avoid affecting the functions of membrane proteins when applying covalent binding techniques. On the other hand, non-covalent binding relies on the unique affinity between specific pairs. For example, biotinylated cells can be immobilized on avidin patterns. Other approaches also allow for the selective immobilization of multiple cell types. For instance, cells modified with single-strand DNA or aptamers can be immobilized onto complementary sequences or proteins due to their unique affinities. Despite the advantages of non-covalent binding, the materials used in this method are vulnerable to degradation in cellular environments.

To address these challenges, I have developed a novel methodology for the programmed immobilization of living cells, guided by following strategy. Firstly, I need to select the independent pairs used for living cells. These pairs must interact effectively within the dynamic cellular environment. Secondly, considering the challenge in manipulating natural living cells, I should devise methods to introduce these pairs onto living cells, while also ensuring they do not affect the function of membrane proteins. In my research, I have pioneered two non-genetic surface modification approaches: metabolic labeling facilitated by click chemistry tools and the introduction of antigen-antibody interactions.

Initially, living cells were labeled with Azide (Az) and (trans-cyclooctene) TCO groups, respectively. The cells were reacted on DBCO, Tetrazine and Methyl coated cover glasses, demonstrating that Az- or TCO-labeled cells could be immobilized in a functional group-dependent manner. Secondly, as for the experiment of introduction of antigen-antibody interactions, azido-phenylalanine (AzF) was introduced to the Anti-mCherry variable domains of heavy chain-only antibodies (VHH) and Anti- emerald green fluorescent protein (EmGFP) VHH, which was successfully

immobilized on Dibenzocyclooctyne (DBCO)-coated glass via click reaction. When conjugated to DBCO substrates, these VHHs enabled specific recognition of mCherry and EmGFP proteins. Similarly, the anti-mCherry VHH-coated substrate resulted in increased immobilization of mCherry-expressing cells on the VHH substrate, while normal HeLa cells did not adhere. This study further explored cell-cell immobilization using Alkyne labeled GFP-HeLa cells conjugated with Anti-mCherry VHH(AzF) through a click reaction. Soft or rigid peptide spacers between VHH and AzF were tested, where both spacers enhanced cell immobilization to the target cells, mCherry expressing HeLa. VHH constructs with peptide spacers proved beneficial for programmed cell immobilization, offering potential applications in targeted cell therapies and tissue engineering. These methods enable selective cell adhesion, achieving patterned cell organization on different surfaces and layers.

This work in programmed immobilization marks a significant advancement in pharmaceutical research. By facilitating precise deposition of living cells onto target cells and patterns, it opens new avenues for research and innovation in pharmaceutical research, bioanalytics, and regenerative medicine. It exemplifies how a nuanced understanding and application of cell immobilization can lead to breakthroughs in biotechnology, enhancing our ability to manipulate and utilize living cells in various scientific and medical applications.

Chapter 1. Programmed immobilization of living cells modified with click reactive functional groups

1.1 Introduction

Over the last decade, therapeutic devices incorporating living cells or tissues have been intensively investigated for applications in tissue engineering and regenerative medicine. Cell adhesion is a key challenge in the development of microdevices and sensors for functional investigation [1,2], tissue remodeling [3], and 3D cell culture [4]. Many biological processes are governed by spatially dependent signals. Programmable immobilization on materials is crucial for manipulating multiple cell types and is promising for therapeutic devices. Controlling the spatial placement of molecules on a surface or across a material may be useful in tissue engineering because it can be used to regulate the topography and geographical distribution of subsequent cell deposition [5].

Several methods have been devised to alter the cell surface for programmed cell immobilization including (1) covalent conjugation to natural terminal groups of cell-surface proteins such as -SH or -NH_2 [6], (2) metabolic labeling of unnatural terminal groups of cell-surface proteins such as the azide group present on the cell surface [7], and (3) hydrophobic interaction with the lipid bilayer membrane of cells [8]. These approaches have led to the development of several therapeutic platforms, including neuron-stem-cell based systems to control NSC (neural stem cell) differentiation [9], mammary-epithelial-cell based three-dimensional tissue-like structures [10], primary-human-astrocytes based single-cell resolution 3D tissue constructs [11], and 2D or 3D microbial organisms [12]. Francis et al. [13] employed single-stranded DNA to achieve cell-programmed immobilization on materials because DNA has a high affinity for complementary sequences on materials and is relatively easy to produce and change; however, there are certain drawbacks to DNA-programmed immobility. When used *in vivo* or in another bioenvironment, the dependability of the immobilization may be affected. Furthermore, this necessitates the creation of optimum oligonucleotide sequences using non-complementary sequences.

The biocompatibility of the click chemical reaction has been demonstrated, and the reactions may occur at physiological pH and temperatures under aqueous conditions. Biorthogonal chemistry, based on inverse electron-demand Diels–Alder cycloaddition, features rapid reaction rates without the need for catalysts. One of the most common bio-orthogonal reactions is the strain-promoted azide-alkyne cycloaddition (SPAAC), which includes Dibenzocyclooctyne (DBCO) -azide [14,15]. SPAAC produces stable triazoles in aqueous solutions without the need for auxiliary reagents such as copper. Furthermore, the Trans-Cyclooctene (TCO)-tetrazine combination displays ultrafast kinetics, selectivity, and long-term water stability [16].

It is also crucial to determine how the reactive functional groups can be obtained on the cell surface. The

metabolic labeling of cells with synthetic sugar analogs has become appealing for the insertion of orthogonal chemical groups into glycoproteins [7,17]. There are three phases in this procedure. N-Azidoacetylmannosamine-tetraacylated (Ac_4ManNAz) enters the cell or organism plasma membranes, is deacetylated by intracellular esterases, and is then incorporated into proteins or lipids through glycan biosynthetic processes. The click reaction or Staudinger ligation allows Ac_4ManNAz to covalently bind to alkynes on the cell membrane [18].

I present a simple method to selectively manage the adherence of two cell types on various patterned surfaces and cell layers by utilizing metabolic labeling and click chemistry tools to realize the idea of patterned cell organization. In this study, I examined whether cell immobilization via click chemistry works on cover glasses and cell layers. HeLa cells expressing green fluorescent protein (GFP) or red fluorescent protein (RFP) were metabolically labeled with azides. TCO-labeled RFP cells were created by reacting azide cells with DBCO-PEG_{12}-TCO (Fig. 1b). In contrast, cover glasses were coated with DBCO, tetrazine, or methyl-polyethylene glycol (mPEG) (Fig. 1a). Finally, functional group-specific immobilization of the cells was assessed. In addition, for cell immobilization on cell layers, tetrazine- or azide-labeled RFP cells were employed in tetrazine-, DBCO-, or azide-labeled GFP cell layers, and comparable cell immobilization on the corresponding cell layers was observed (Fig. 1c).

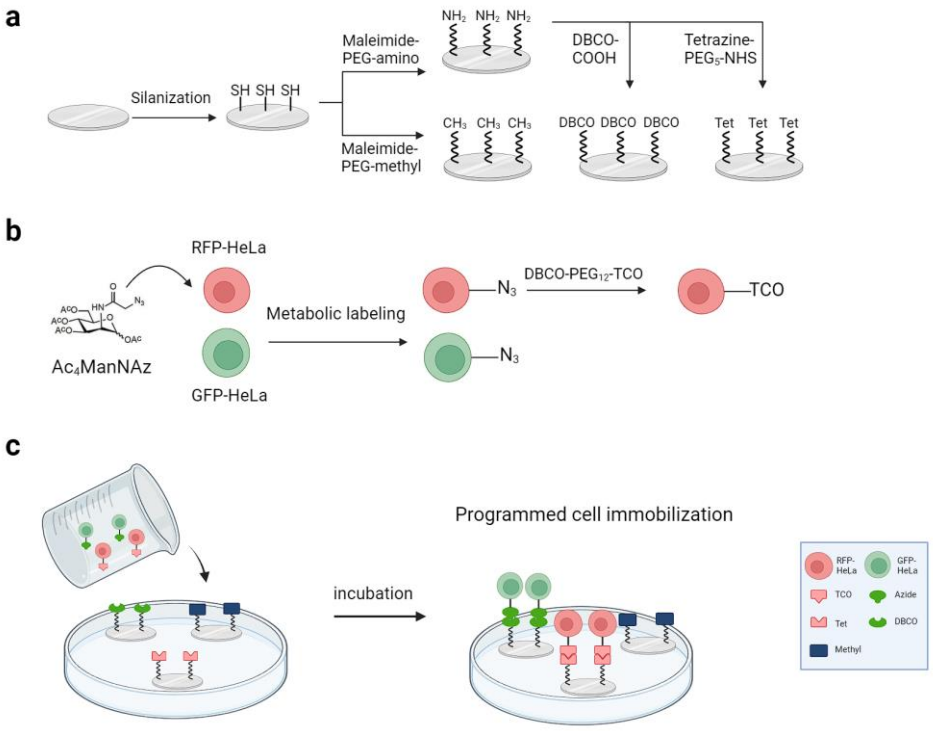

Fig. 1. Schematic representation of programmed immobilization of living cells

a) Cover glasses were silanized with thiol ligands. Subsequently, they were treated with maleimide-PEG-amino or maleimide-PEG-methyl to add amino or methyl groups. Lastly, the glasses with amino groups were further modified with DBCO or Tetrazine, respectively. b) RFP-HeLa and GFP-HeLa cells were labeled with Ac_4ManNAz to generate Az-labeled cells. Then Az-RFP-Hela were incubated with DBCO-PEG_{12}-TCO to generate TCO-RFP-HeLa. c) Az-GFP-HeLa and TCO-RFP-HeLa were incubated in a culture dish in which three different cover glasses, DBCO-, Tetrazine-, or methyl-coated, were added. Az- or TCO-labeled cells could be immobilized in a functional group-dependent manner.

1.2 Materials and Methods

Materials

Cover glass (φ13 mm) was purchased from Matsunami Glass Co. Ltd. (Osaka, Japan). NH_3 (28%), H_2O_2 (20%), H_2SO_4 (98%), EtOH (99.5%), penicillin/streptomycin (1% each), dimethyl sulfoxide, Accutase and Dulbecco's Phosphate Buffered Saline (D-PBS(-)) were purchased from Nacalai Tesque, Inc. (Kyoto, Japan). (3-Mercaptopropyl) trimethoxysilane (MPTMS) was purchased from Shin-Etsu Chemical Co. (Tokyo, Japan). Calcein-AM was purchased from Dojindo (Kumamoto, Japan). NH_2-PEG-maleimide (MW = 2000) and mPEG-maleimide (MW = 2000) were purchased from Creative PEGWorks (Chapel Hill, NC, USA). TCO-PEG_{12}-DBCO, tetrazine-PEG_5-NHS, Cy5-TCO, and Cy3-tetrazine are purchased from Click Chemistry Tools (Scottsdale, AZ, USA); Ac_4ManNAz, calcein Red-Orange AM, and fetal bovine serum (FBS) were purchased from Thermo Fisher Scientific (Waltham, MA, USA); DBCO-Texas Red and azide-Texas Red were purchased from Jena BioScience (Jena, Germany). 4-(4,6-dimethoxy-1,3,5-triazin-2-yl)-4-methylmorpholinium chloride (DMTMM) and DBCO-COOH were purchased from Sigma-Aldrich (St. Louis, MO, USA); Low-glucose D-MEM with L-glutamine and Phenol Red was purchased from Wako Pure Chemical Industries, Ltd. (Osaka, Japan). Twenty-four-well plates, 96-well plates, 10 cm dishes, and 8-well chamber slides were purchased from Corning (Corning, NY, USA). HeLa, green fluorescent protein-HeLa (GFP-HeLa), and red fluorescent protein-HeLa (RFP-HeLa) cells were obtained from Anti-Cancer Japan (Chiba, Japan); Cell Dissociation Buffer, enzyme-free, Hanks' Balanced Salt Solution was purchased from Gibco (Waltham, MA, USA); Sialidase (10269611001, Roche) was purchased from Merck (Darmstadt, Germany)

Methods

Cover glass coating

Cover glasses (13 mm) were soaked in 140 mL of NH_3:H_2O_2:water, 20:20:100 (v/v), for 10 min using a glass holder. The cover glasses were then steeped for 120 min in 160 mL of H_2O_2:98% H_2SO_4, 40:120 (v/v), in Teflon-coated ware, washed twice with double-distilled water, and ultrasonically soaked twice in EtOH for 3 min. The cover glass substrates were silanized in 24-well plates for 24 h in 1% MPTMS in 99.5% EtOH at 20 °C, followed by two washes with ultrasonication in EtOH for 3 min. Cover glasses were reacted in 2 mg/mL of NH_2-PEG-maleimide (MW = 2000):methyl-PEG-maleimide (MW = 2000), 30:70 (w/w), or methyl-PEG-maleimide (MW = 2000) in D-PBS(-) (pH 7.4) at 20 °C for 24 h after being heated at 110 °C for 1 h. A corresponding volume of 1.2 mM DBCO-COOH and 3 mM DMTMM was then dissolved in D-PBS(-) for 15 min using ultrasonication. At 20 °C, NH_2-PEG-coated cover glasses were reacted with 0.5 mL of DBCO-COOH and

DMTMM or 0.6 mM tetrazine-PEG_5-NHS in D-PBS(-) for 4 h. The cover glasses were then cleaned twice with 1 mL of D-PBS(-). TCO-Cy5 or azide-Texas Red in D-PBS(-) (10 μM) were reacted on cover glasses for 10 min to detect tetrazine or DBCO, followed by washing twice with 1 mL D-PBS(-).

Cell modification with click ligands

Cells were seeded on a 10 cm dish at a concentration of 2×10^5 cells/mL in 10 mL of DMEM with 10% (v/v) FBS and 1% (v/v) penicillin/streptomycin and cultured for 24 h. The culture medium was replaced with 40 μM Ac_4ManNAz in DMEM with 10% FBS and 1% penicillin/streptomycin and incubated for 48 h. For TCO modification, azide-labeled cells were incubated in 40 μM TCO-PEG_{12}-DBCO in DMEM with 10% FBS and 1% penicillin/streptomycin for 40 min followed by washing with 1 mL of D-PBS(-). Then, 1 mL of Accutase was added to detach the cells and collect the cell suspension in DMEM with 10% FBS and 1% penicillin/streptomycin.

To modify the tetrazine groups in the cell suspension, RFP HeLa cells were seeded on a 10 cm dish and cultured for 24 h. The culture medium was replaced with 40 μM Ac_4ManNAz in DMEM and incubated for 48 h. Cells were then removed using Accutase and either 10 mL of DMEM for the control group or 40 μM tetrazine-PEG_{12}-DBCO in DMEM for the treatment group was used to resuspend the cells. The cell concentration in both groups was 1×10^5 cells/mL. Finally, both groups were incubated in a MACSmix Tube Rotator at 4 ℃ for 2 h.

Detecting the azide or TCO functional group on cell surfaces

Cells were seeded in an 8-well chamber at a concentration of 1×10^4 cells/mL in 0.5 mL culture medium and cultured for 24 h. The culture medium was replaced with 40 μM Ac_4ManNAz in DMEM, and the cells were incubated for 48 h. For the untreated group, the medium was replaced with DMEM without Ac_4ManNAz. The cells were washed with 1 mL D-PBS(-). To confirm azide tagging, the cells were incubated with 10 μM DBCO-Texas Red for 10 min, followed by washing with 1 mL of D-PBS(-).

For TCO modification, azide-labeled cells were incubated in 40 μM TCO-PEG_{12}-DBCO in DMEM for 40 min followed by washing with 1 mL of D-PBS(-). To confirm TCO modification, cells were reacted with 10 μM tetrazine-Cy3 for 10 min followed by washing with 1 mL of D-PBS(-). For RFP-HeLa cell suspension modification with tetrazine-PEG_{12}-DBCO, RFP HeLa cells were seeded in a 10 cm dish and cultured for 24 h. The culture medium was replaced with 40 μM Ac_4ManNAz in DMEM and incubated for 48 h. Cells were removed using Accutase and were then resuspended at a concentration of 1×10^5 cells/mL in either 10 mL of DMEM for the control group or 40 μM tetrazine-PEG_{12}-DBCO in DMEM for the treatment group. Then, both groups were incubated in a MACSmix Tube Rotator at 4 ℃ for 2 h. Tetrazine modification was evaluated by flow cytometer analysis after reacting with TCO-AF488. Cell viability was assessed using the WST-8 assay.

Cell immobilization on cover glasses

DBCO-, tetrazine-, or methyl-PEG-coated cover glasses were placed in 24-well plates. After harvesting cells with Accutase, 0.5 mL of 1 × 10^6/mL TCO- or azide-labeled cells were added on the cover glasses in the well plate and incubated at 37 ℃, 5% CO_2 for 30 min. To prevent non-specific adhesion, the culture medium was replaced with 0.5 mL EDTA cell dissociation buffer in enzyme-free Hanks' balanced salt solution, followed by incubation at room temperature for 5 min. The cover glasses were then washed twice with 1 mL of D-PBS(-). To verify immobilization via sialic acid, cells were treated with sialidase (50mU, 500 μL final volume) in sialidase buffer (25 mM HEPES, pH 6.75, 150 mM NaCl), or in sialidase buffer alone (control cells) at 37 ℃, 5% CO_2 for 50 min after azide-labeled cells immobilized on DBCO coated cover glasses.

Cell-selective immobilization on cover glasses

DBCO-, tetrazine-, and methyl-PEG-coated cover glasses were placed in one well of a 6-well plate. For selective immobilization, a 2.4 mL mixture of azide-GFP and TCO-RFP cells (1 × 10^6 cells/mL of each) was added to the cover glass in the well plate. To prevent non-specific adhesion, the culture medium was replaced with 0.5 mL EDTA cell dissociation buffer in enzyme-free Hanks' balanced salt solution, followed by incubation at room temperature for 5 min. The cover glasses were then washed twice with 1 mL of D-PBS(-).

Quantitative evaluation of immobilized cells in cell immobilization and cell-selective immobilization

For cell immobilization, cells were labeled with calcein-AM before harvesting with Accutase, and then incubated with 2 mM calcein-AM in D-PBS(-) for 15 min, followed by washing with 1 mL of D-PBS(-). For cell-selective immobilization, before harvesting cells with Accutase, azide-labeled HeLa cells were incubated with 2 mM calcein-AM in D-PBS(-), and TCO-labeled HeLa cells were incubated with 2 mM calcein-red-orange-AM in D-PBS(-) for 15 min, followed by washing with 1 mL of D-PBS(-). After incubation on cover glasses, the cells were lysed with lysis buffer for 15 min. Fluorescence intensity was measured after centrifuging the lysate at 12000 × g at 4 ℃ for 20 min.

Cell-cell immobilization by Tet-TCO conjugation

Green fluorescent protein-expressing HeLa cells were seeded in 4-well chambers at a concentration of 4 × 10^4 cells/mL in 1 mL of DMEM, whereas RFP HeLa cells were seeded in 10 cm dishes at a concentration of 1 × 10^6 cells/mL in 10 mL of DMEM. The TCO-PEG_{12}-DBCO modification for GFP cells and tetrazine-PEG_{12}-DBCO modification for RFP cells are described above. The TCO-GFP or azide-GFP cells were then incubated with 700 μL TCO-RFP cell suspension (cell concentration = 1 × 10^6 cells/mL) for 15 min at 37 °C. Free cells were removed using enzyme-free Hanks' solution with 10% FBS at a vibration frequency of 350 rpm on a multi-shaker (AS-ONE MS-300).

Green fluorescent protein-expressing HeLa cells were seeded in 4-well chambers at a concentration of 4 × 10^4 cells/mL in 1 mL of DMEM, whereas RFP HeLa cells were seeded in 10 cm dishes at a concentration of 1 × 10^6 cells/mL in 10 mL of DMEM and cultured for 24 h. The culture medium was replaced with 40 μM Ac_4ManNAz in DMEM and incubated for 48 h. For DBCO modification, GFP cells were washed with 1 mL D-PBS(-) and treated with 40 μM TCO-PEG_{12}-DBCO in DMEM for 40 min, followed by washing with 1 mL D-PBS(-). Thereafter, DBCO-GFP or azide-GFP cells were incubated with 700 μL azide-RFP cell suspension (cell concentration = 1 × 10^6 cells/mL) for 15 min at 37 ℃. Free cells were removed using enzyme-free Hanks' solution with 10% FBS at a vibration frequency of 350 rpm on a multi-shaker (AS-ONE MS-300).

1.3 Results

1.3.1 Tetrazine-PEG or DBCO-PEG is coated on cover glasses

The cover glass coating was visualized using a fluorescent dye. A fluorescence signal was obtained after reacting with Cy5-TCO on the tetrazine-PEG-coated cover glass, but not on the methyl-PEG-coated cover glass (Fig. 2a). The covalent reaction of azide-Texas Red with DBCO- or methyl-PEG-coated cover glass yielded similar results (Fig. 2b).

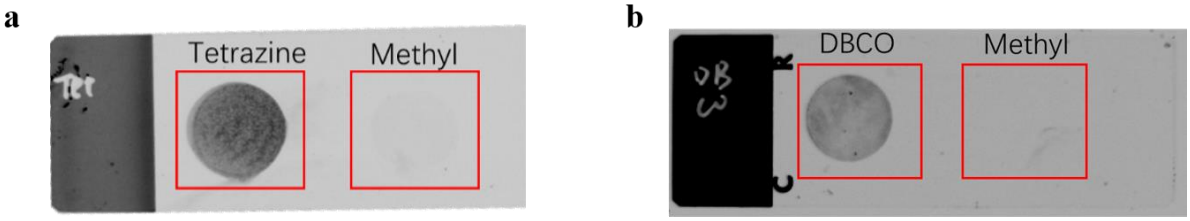

Fig. 2. Confirmation of cover glass coating with tetrazine-PEG and DBCO-PEG

After tetrazine-PEG (a) or DBCO-PEG (b) was incubated with Cy5-TCO or Texas Red-Azide, respectively, fluorescence images were taken with ImageQuant™ LAS 4000. Exposure time = 2 ms

1.3.2 GFP HeLa cells are labeled with azide or TCO

After incubation with or without Ac_4ManNAz, the GFP-HeLa cells were treated with DBCO-Texas Red. Texas Red fluorescence was detected in Ac_4ManNAz-treated GFP-HeLa cells (Fig. 3a) but not in untreated GFP-HeLa cells (Fig. 3b). These results indicate that the azide group was present on the surface of HeLa cells

after metabolic labeling with $Ac_4ManNAz$.

Cell TCO modification was detected using tetrazine-Cy3. Cy3 fluorescence was confirmed in DBCO-PEG-TCO-treated azide-GFP-HeLa cells (Fig. 3c) but not in DBCO-TCO-treated GFP-HeLa cells (Fig. 3d). These findings demonstrate the successful sequential introduction of azide followed by TCO functional groups to the cell membrane. If free azide groups remain on the TCO cells, orthogonal selectivity may be impeded. However, free azide groups were not observed on the TCO cells when DBCO-PEG-TCO-treated azide-GFP-HeLa cells were incubated with DBCO-Texas Red (Fig. 3e).

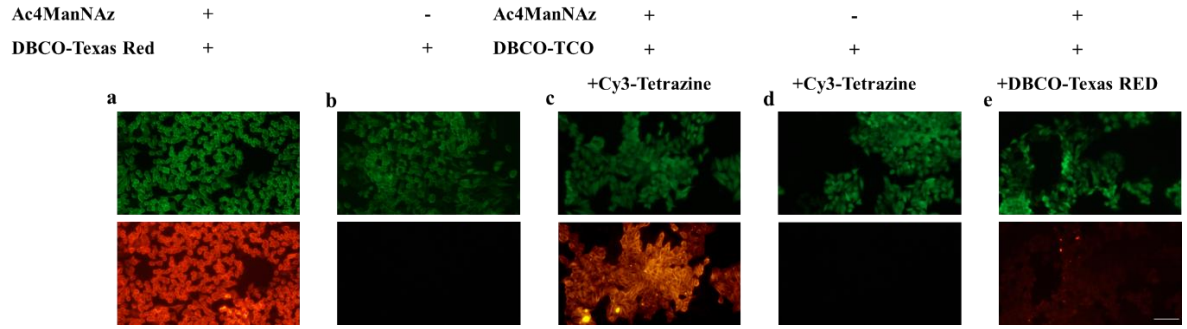

Fig. 3. Confirmation of GFP HeLa cells labeling with azide or TCO

GFP Hela cells were incubated in the presence or absence of $Ac_4ManNAz$, and then incubated with DBCO-Texas Red. Azide-labeled cells were incubated in the presence or absence of DBCO-PEG-TCO, followed by incubation with Cy3-tetrazine or DBCO-Texas Red. The cells were observed under a fluorescence microscope (Olympus IX73) with an FITC (upper) or TRITC (lower) filter. Scale bar = 100 μm

1.3.3 Azide and TCO cells are immobilized on the cover glass via corresponding click chemistry pairs

Azide/DBCO and TCO/tetrazine are orthogonal and covalent click chemistry pairs, respectively. Many more cells were immobilized on the DBCO-PEG-coated cover glasses than on the control surface (Fig. 4a, 4b). This result underscores the successful immobilization of azide cells on the DBCO-coated cover glass, exhibiting minimal non-specific binding. Furthermore, the density of the immobilized azide cells increased with increasing initial cell numbers and plateaued when more than 2×10^6 cells/mL were added to the wells with cover glasses (Fig. 4c). A similar trend was observed for the pair of TCO-modified cells and tetrazine-coated cover glasses (Fig. 4d, 4e, 4f). Given the hydrophobic nature of DBCO, to confirm the specificity of cell adhesion to DBCO-coated cover glasses, both Az-labeled cells and untreated cells were introduced onto DBCO-coated cover glasses. Remarkably, a substantial presence of Az-labeled cells was observed on the DBCO surface, while only a minimal number of untreated cells remained (Fig. 4g). Furthermore, a significant reduction in immobilized Az-labeled cells on DBCO-coated cover glasses following sialidase treatment indicated that $Ac_4ManNAz$ had been metabolically incorporated into the cell membrane as sialic acid. This incorporation led to the detachment of Az-labeled cells from the DBCO surface since the Az groups on the cell membrane were removed by sialidase (Fig. 4h). These results collectively demonstrate that the immobilization of Az-labeled cells onto DBCO-coated glasses

occurs via specific click pairs rather than non-specific adhesion.

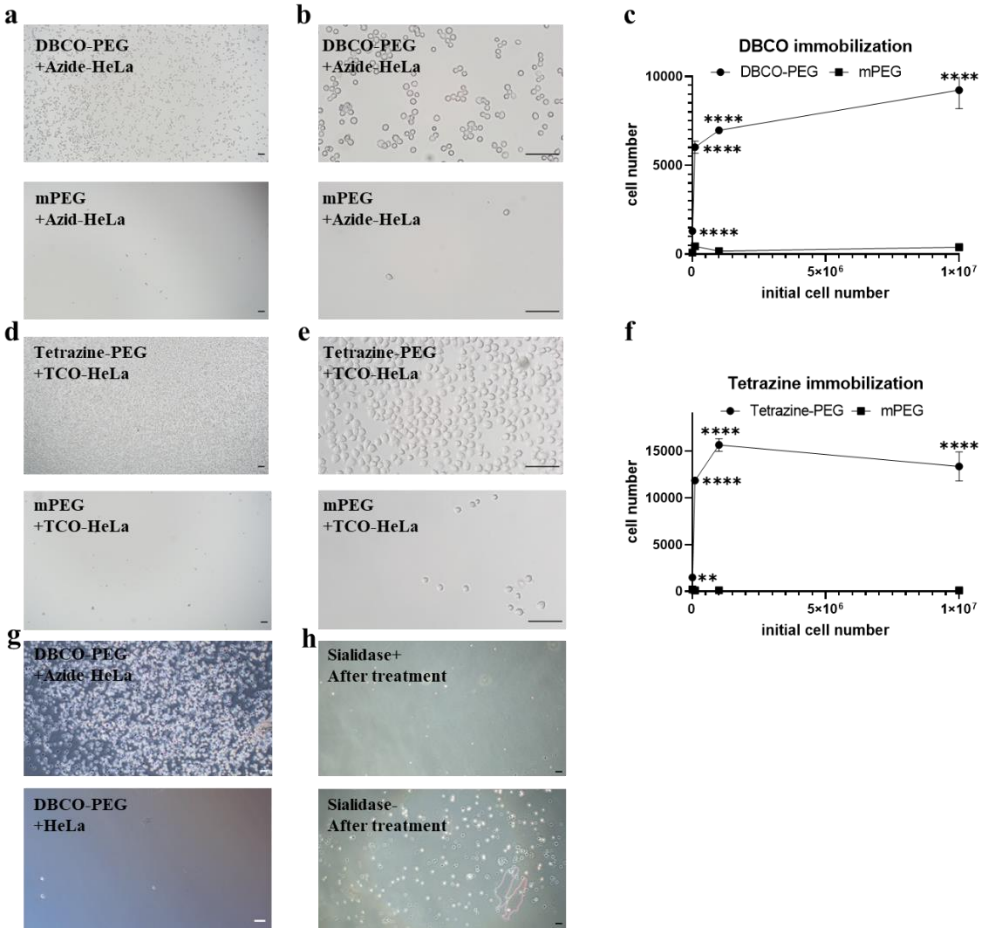

Fig. 4. Immobilization of azide-labeled cells on DBCO-PEG-coated cover glasses and TCO-labeled cells on tetrazine-PEG-coated cover glasses

Azide-labeled cells were incubated on DBCO-PEG-coated (a) and methyl-PEG (mPEG)-coated (b) cover glasses and TCO-labeled cells were incubated on tetrazine-PEG-coated (d) and mPEG-coated (e) cover glasses. (g) azide-labeled cells or non-treated cells were incubated on DBCO-PEG-coated cover glasses. (h) After azide-labeled cells immobilized on DBCO-PEG-coated cover glasses, cells were treated with or without sialidase. TD images were taken using an Olympus X73 microscope with 4× (a, d, g, h) or 20× (b, e) objective lens. Scale bar = 100 μm. (c, f) Azide- and TCO-labeled cells were stained with calcein-AM and incubated on DBCO-, tetrazine- or mPEG-coated cells at concentrations of 0.001, 0.01, 0.1, or 1 × 10^7 cells/well. Cells were lysed with lysis buffer after washing with EDTA followed by D-PBS(-). The fluorescence intensity of the cell lysate was measured with a microplate reader. The cell number was calculated from the standard curve. Each result represents the mean ± S.D and is performed in T-test. **** $P < 0.0001$

1.3.4 Selective immobilization on cover glass in azide- or TCO-labeled cell mixtures

To verify selective cell immobilization via the orthogonal click reaction, a mixture of azide-GFP cells and TCO-RFP cells were incubated on DBCO-, tetrazine-, and methyl-PEG-coated cover glasses. Azide-GFP or

TCO-RFP cells were observed only in the DBCO- (Fig. 5a) or tetrazine-PEG coated cover glasses (Fig. 5b), respectively. Cross-reaction of azide-GFP cells with tetrazine-PEG-coated cover glass was hardly observed (Fig. 5a). The same result was obtained using a combination of TCO-RFP cells and DBCO-PEG-coated cover glasses (Fig. 5b). Both azide- and TCO-labeled cells were hardly observed on the mPEG-coated cover glasses (Fig. 5c). Selective immobilization was demonstrated by quantitative evaluation using calcein-AM-labeled azide cells and calcein-red-orange-labeled TCO cells. Calcein-AM fluorescence signals were exclusively detected on the DBCO-coated cover glass surfaces, whereas calcein-red-orange-labeled TCO cells exhibited fluorescence signals solely on the tetrazine-PEG-coated cover glass. Notably, minimal non-specific cell binding was observed on the mPEG-coated surface (Fig. 5d).

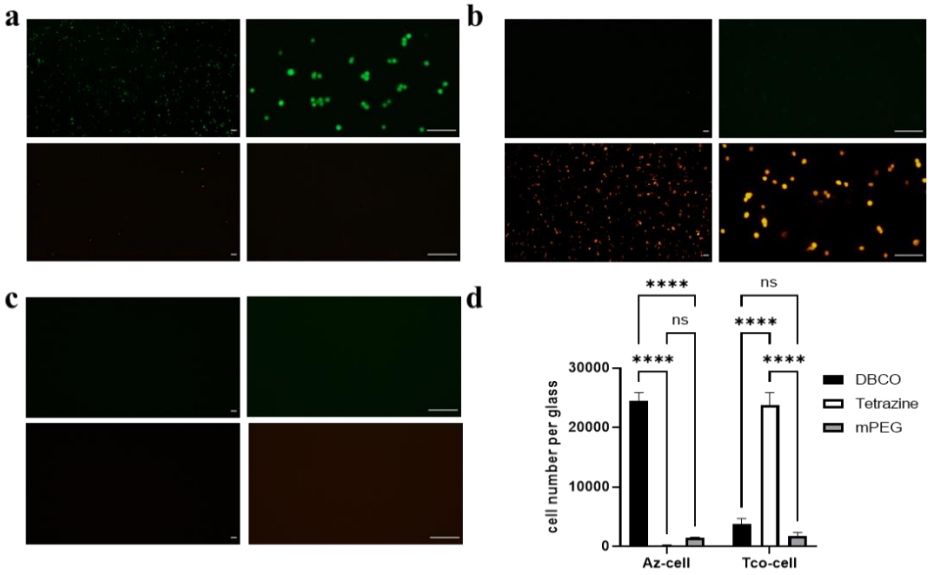

Fig. 5. Selective immobilization of azide- or TCO-labeled cells on DBCO- or tetrazine-PEG-coated cover glasses

The mixture of Az-GFP cells and TCO-RFP cells (1×10^6 cells/well) were incubated on DBCO- (a), tetrazine- (b) and mPEG- (c) coated cover glasses. Cells were washed with EDTA followed by D-PBS(-). Fluorescence images were taken by fluorescence microscope with an FITC or TRITC filter and 4× or 20× objective lens. Green = Azide-GFP HeLa. Red = TCO-RFP HeLa. Scale bar = 100 μm. D) Azide- and TCO-labeled cells were stained with calcein-AM and calcein-red-orange-AM, respectively. A mixture of Az-GFP and TCO-RFP cells (1 × 106 cells/well) was incubated on DBCO-, tetrazine-, and mPEG-coated cover glasses. Cells were lysed with lysis buffer after washing with EDTA followed by D-PBS(-). The fluorescence intensity of the cell lysate was measured with a microplate reader. The cell number was calculated from the standard curve. Each result represents the mean ± S.D and is performed in one-way ANOVA test. **** $P < 0.0001$

1.3.5 Immobilization of azide- or TCO-labeled cells on the cell layer

To validate cell immobilization on the cell layer via the click reaction, tetrazine-RFP cells were incubated

on the TCO- or azide-modified GFP cell layer. A large number of tetrazine-modified RFP cells were immobilized on the TCO-modified GFP cell layers (Fig. 6a, 6f) but rarely on the azide-modified cell layers (Fig. 6b). Additionally, 3D reconstructed images based on slices indicated the positioning of RFP cells on GFP cells (Fig. 6c). This revealed that the TCO cells were immobilized on the corresponding modified cell layer. When the DBCO-azide click pair was switched, the Azide-RFP cells were immobilized on the DBCO-GFP cell layer (Fig. 6d, 6g) not on the Azide-GFP cell layer (Fig. 6e).

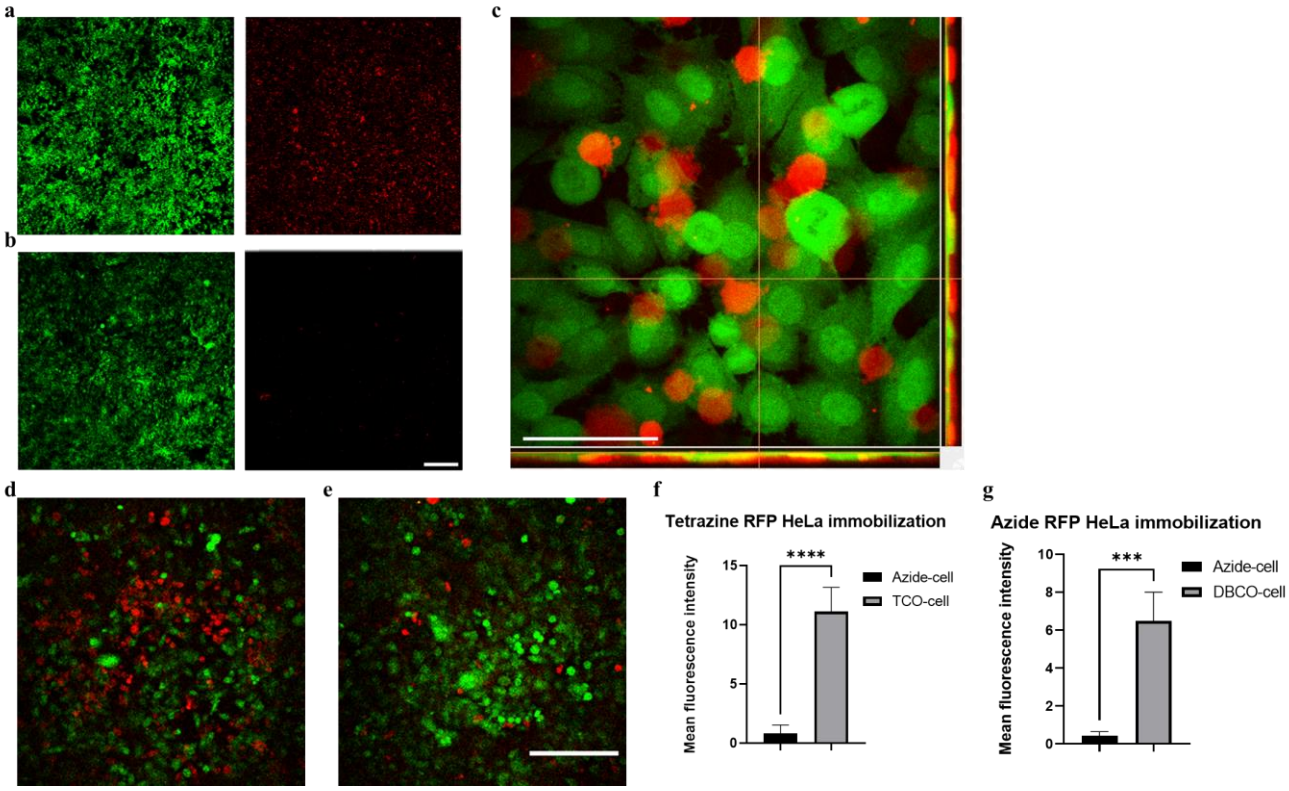

Fig. 6. Cell-cell immobilization by Tet-TCO conjugation or DBCO-azide conjugation

GFP HeLa cells were modified with TCO (a) or $Ac_4ManNAz$ (b) and were then treated with Tet-modified RFP HeLa for 15 min. Immobilized Tet-RFP-HeLa cells were detected. The X-Z/Y-Z image (c) taken with a 40× objective lens validates this result. Similar outcomes were observed when azide-RFP cells were immobilized on DBCO-GFP (d) or azide-GFP cells (e). Scale bar = 100 μm. f) Mean fluorescence intensity of immobilized tetrazine labeled RFP HeLa cells on TCO (treatment) or Azide (control) labeled GFP HeLa cells. g) Mean fluorescence intensity of immobilized Azide labeled RFP HeLa cells on DBCO (treatment) or Azide (control) labeled GFP HeLa cells. Each result represents the mean ± S.D and is performed in T-test. **** $P < 0.0001$. *** $P < 0.001$.

1.4 Discussion

To demonstrate the assistance of orthogonal click chemistry pairs in selective cell immobilization, I employed click pairs on the surfaces of cells or cover glasses. Azide-labeled HeLa cells were immobilized on a DBCO-coated surface, with few cells on the mPEG-coated surface; TCO-labeled cells had the same outcome

with tetrazine-coated or mPEG-coated surfaces (Fig. 4). Adding a mixture of TCO- and azide-labeled cells to the DBCO/tetrazine/mPEG cover glass combination also resulted in excellent bio-orthogonal immobilization between the complement cells and surface pairings (Fig. 5). Karver et al. [19] developed two cell line platforms with abundant TCO and DBCO on cell surfaces. Using AF750-TET and AF647-Azide, they demonstrated that tetrazine-TCO and azide-DBCO reactions were independent of the bio-orthogonal labeling of two different living cell populations in the same culture. In the present study, I succeeded in the biological application of the excellent bio-orthogonality of click chemistry. My research may contribute to the creation of cell arrays based on design patterns that are important for tissue reengineering, cell spatial-temporal studies, living cell-based sensors, and other applications in future. Single-stranded DNA (ssDNA) promises selectivity in cell patterning; however, various limitations still exist regarding its broader utility. For example, the degradation of ssDNA by nucleases occurs in culture media with serum during long-term culture [20]. In addition, designing multiple pairs of sequences is challenging. The optimal annealing temperatures for ssDNA typically exceed 60 ℃, making it unsuitable for cellular applications that operate at 37 ℃ or below [21]. Additionally, the large amount of DNA on the cell surface may stimulate immune cells in a manner similar to that of neutrophil extracellular traps involving Toll-like receptors in vivo [22]. These challenges collectively restrict the widespread application of ssDNA in cellular contexts.

Cell metabolic labeling with Ac_4ManNAz is widely used for living cell imaging and cell surface engineering [17], and numerous studies have shown that two days of treatment with a low concentration of Ac_4ManNAz in Hela cells results in permissive cytotoxicity. Hong et al. [23] showed 100% Hela cell viability when employing 50 μM Ac_4ManNAz for 2 days. Haga et al. [24] demonstrated that metabolic labeling with 25 μM and 50 μM Ac_4ManNAz on Hela cells for 48 h results in 93% and 87% viability, respectively, whereas the high concentration group (100 M) only had 70% viability. The results of an MTT assay by Yuan et al. [25] showed that Hela cells retained nearly 95% viability when incubated with up to 50 μM Ac_4ManNAz for 2 days. Therefore, I chose 40 μM over 2-day incubation period in the present study. Furthermore, after azide labeling and subsequent TCO modification, the cell viability was maintained at 82% (data not shown). These results suggest that click ligand labeling causes minimal damage to living cells. However, the effects of metabolic labeling on cellular functions remain a concern. To address this question, Han et al. [26] demonstrated that when A549 cells were treated with 50 μM Ac_4ManNAz, the expression level was altered by more than 5-fold in only 4.9% of 2047 genes. Altered gene expression is linked to cellular functions, such as the urogenital cancer pathway, cellular infiltration, and cell maturation [26]. This finding suggests that most cell functions were less disrupted in my study.

My tool is convenient for achieving multicell patterns in vitro by relying on stable and selective covalent bonds between cells and artificial interfaces. However, the covalent bond between the surface protein and the interface might potentially interfere with processes such as cell proliferation and migration, because disassociation is necessary for these processes [27]. Integrins are extracellular glycoproteins that play a vital role in cell adhesion [28]. During migration and mitosis, cells dissociate through the enzymatic cleavage of integrins [29].

Neu3, a human neuraminidase (sialidase) enzyme localized in the plasma membrane, mediates sialic acid release from glycolipids and glycoprotein substrates [30]. Howlader et al. [31] and Jia et al. [32] demonstrated that the inhibition of Neu3 in several cancer cell lines caused significant retardation of cell migration. Studies have shown a significant reduction in the presence of membrane azide ligands when Ac_4ManNAz-labeled cells were treated with neuraminidase (sialidase) [7,33,34]. Furthermore, when metabolically-labeled cells are treated with tunicamycin, an inhibitor of protein glycosylation, the azide content on the cell surface sharply decreases [7,35]. These results were supported by the fact that the azide ligand of Ac_4ManNAz originates from the sialic acid biosynthetic pathway [33]. These findings indicate that sialic acid is cleaved by neuraminidase even under covalently bonded conditions. In conclusion, immobilizing azide cells on DBCO-coated surfaces does not seem to have a severe influence on their migration and proliferation.

Chapter 2. Programmed immobilization of living cells via antigen – VHH antibody interaction

Antigen-antibody recognition offers robust independence and numerous pairs. Thus, I considered it's potential of introducing antigen-antibody interactions as an alternative for click pairs. In this strategy, site-specific conjugation of antibody, without interfering the antibody's functional integrity, is crucial for following cell immobilization. In this chapter, firstly my efforts were directed towards the conjugation of aligned VHH (variable domain of the heavy chain of heavy-chain) antibodies. Secondly, I explored the possibility of conjugating VHH onto cell membranes, with the goal of facilitating cell-cell stacking.

Section 1. Development of site-specific conjugation of VHH-antibody for effective recognition of antigen on living cells

1.1 Introduction

Biosensors and microdevices using living cells have gained significant impetus in recent years, surpassing those based on molecules. This is due to the fact that devices incorporating living cells provide highly valuable functional information, facilitating studies in cell signaling [36], tissue engineering [37], pharmacology and toxicity [38], as well as the development of precise biosensors [39], among other applications. However, the immobilization of living cells on device surfaces, particularly on chips or electrodes, presents challenges. Additionally, these sensors and microdevices often require specific cell patterns, such as cell arrays [40]. To address the challenges of living cell immobilization, several approaches have been devised. These include covalently binding cells via chemical reactions [6,7], cell entrapment in biocompatible materials [41], physical adsorption [42], and cell capture through antigen-antibody interactions [43]. Among these techniques, cell immobilization on antibody-coated surfaces is attracting more attention. This is because the high-affinity and specific recognition of antibodies with a cell's endogenous antigens achieve labeling-free and selective cell immobilization from cell mixtures [44].

For cell immobilization based on antibody-coated substrates, antibody fixation is a crucial step. Current methods for antibody fixation include absorption [45], covalent binding to the antibody's amino acid residues [46], affinity binding via protein tags [47], and solid-phase (sol-gel) capture [48]. The orientation of antibodies plays a critical role in enhancing the binding capacity during cell immobilization. Typically, random antibody fixation may lead to suboptimal exposure of recognition sites, thereby

diminishing the interaction efficiency. In contrast, oriented immobilization ensures maximal exposure and affinity of the antibody's active sites. Despite the recognized importance of antibody orientation, achieving this with specificity presents considerable challenges, primarily due to the multitude of reactive groups present on antibodies. Current methods for antibody orientation involve diverse strategies. Non-covalent approaches include the utilization of protein G to capture the tail of the antibody [49]. On the covalent front, techniques include site-specific modification of amino acid residues [50], targeting the sugar chains on the Fc region [51], and reactions with protein His tags [52]. In this context, the use of variable domains of heavy chain-only antibodies (VHH) is gaining attention as a more effective alternative to conventional monoclonal antibodies (mAbs). The relatively simple structure and smaller size of VHHs confer higher stability, increased likelihood of epitope binding, and ease of screening and expression, all while maintaining high affinity [53]. However, a notable issue arises with VHHs: the absence of an Fc region and disulfide bond precludes the possibility of site-specific binding of VHHs on substrates, a technique commonly employed with mAbs. This presents a unique challenge in the field of antibody immobilization, necessitating innovative approaches to leverage the advantages of VHHs while overcoming their structural limitations.

The strategic alignment of VHH on substrates, particularly through the integration of nonnatural amino acids, represents a significant advancement in the field of antibody engineering. The introduction of nonnatural amino acids equipped with click ligands into antibodies, including VHH, facilitates bio-orthogonal conjugation [54]. This approach offers high specificity, primarily because these nonnatural amino acids, along with their corresponding aminoacyl tRNA synthetases (aaRS)–transfer RNA (tRNA) pairs, do not interfere with the natural amino acids present in the system [55]. An additional advantage of this method is the ability to position the conjugation site away from the antibody's recognition domain, thereby preserving the antibody's inherent binding functionality. VHH, in particular, maintains binding abilities and specificity that are comparable to traditional full-length monoclonal antibodies or single-chain variable fragments (scFvs) [56]. This is a significant observation, as it indicates that the incorporation of nonnatural amino acids into VHH does not detract from their performance. Importantly, such modifications do not compromise the expression, solubility, or stability of nanobodies, even when compared to full-length mAbs [57,58]. This aspect is crucial, as it ensures that the enhanced properties of the nanobodies due to the nonnatural amino acids do not come at the cost of their fundamental characteristics. Overall, the strategic use of nonnatural amino acids in VHH conjugation opens up new avenues in the development of highly specific and efficient biosensors and therapeutic agents.

In this study, I explored the alignment of azido-phenylalanine (AzF)-incorporated VHH antibodies to improve cell immobilization. Initially, azido-phenylalanine was introduced to a fluorescent protein, monomeric Kusabira-Orange 2 (mKO2). The mKO2-AzF was immobilized on the DBCO-coated glass within 30 min of reaction, while mKO2 without AzF incorporation remained unbound. These findings demonstrate that DBCO on the substrate enables immobilization AzF tagged proteins. Anti-mCherry

VHH and Anti-emerald green fluorescent protein (EmGFP) VHH, with Az introduced at the C-terminus, distal to its antigen-binding site for the mCherry and EmGFP, were expressed and purified in *Escherichia coli*. Through a GST-tag, mCherry was bound to resin, and VHH was then added. The bound and unbound fractions obtained after the addition of glutathione were analyzed using SDS-PAGE. Bands for both mCherry and VHH were observed in the bound fraction but not in the unbound fraction, confirming the binding of VHH to mCherry. And Anti-EmGFP VHH yields similar results. Following the conjugation of both VHH-AzF to the DBCO substrate, a mixture of mCherry and EmGFP proteins was applied to the surface. Each protein selectively adhered to its complementary VHH. Finally, HeLa cells expressing mCherry on their surfaces (mCherry-coated cells) were incubated with an anti-mCherry VHH-coated substrate for 1 h. This resulted in increased immobilization of mCherry-coated cells on the VHH substrate, while normal HeLa cells did not adhere.

1.2 Materials and methods

Materials

Escherichia coli BL21(DE3) was purchased from BioDynamics Laboratory, Inc. (Tokyo, Japan). Φ13 mm glass was purchased from Matsunami Glass Ind., Ltd. (Tokyo, Japan). NH_2-PEG-maleimide (MW = 2000) and mPEG-maleimide (MW = 2000) were purchased from Creative PEGWorks (Chapel Hill, NC, USA). (3-Mercaptopropyl) trimethoxysilane (MPTMS) was purchased from Shin-Etsu Chemical Co. (Tokyo, Japan). Arginine Hydrochloride (Arg·HCl), Accutase, COSMOGEL GST-Accept, Hydrogen chloride, LB medium, 4-(2-hydroxyethyl)-1-piperazineethanesulfonic acid (HEPES), Dulbecco's Modified Eagle Medium (DMEM), Penicillin-Streptomycin-Glutamine (PSG), Sucrose, paraformaldehyde, Isopropyl-β-d-thiogalactopyranoside (IPTG), and trypsin were purchased from Nacalai Tesque (Kyoto, Japan). H-Phe(4-N_3)-OH(AzF) was purchased from Watanabe Chemical Industries, Ltd. (Hiroshima, Japan). High-pressure homogenizer (EmulsiFlex-B15) was purchased from AVESTIN (Ottawa, Canada). TALON metal affinity resin was purchased from Takara Bio (Shiga, Japan). 48-well, 24-well, 12-well, and 6-well plates were purchased from Corning (NY, USA). Ultrafree-MC, HV, 0.45 μm and Amicon ultra 15, 10 kDa MWCO were purchased from Millipore Co. (Massachusetts, US). DBCO-PEG_4-5/6-FAM and 5/6-Texas Red-PEG_3-Azide were purchased from Jena BioScience (Jena, Germany). D-PBS(-) was purchased from Nissui (Tokyo, Japan). Ni Sepharose 6 Fast Flow was purchased from Cytiva (Massachusetts, US). 96-well plate Greiner was purchased from Bio-One (Kremsmuenster, Austria). FuGENE 6 was purchased from Promega (Wisconsin, US). Opti-MEM Reduced Serum Medium was purchased from Gibco (Massachusetts, US). Anti-mCherry-Rabbit IgG (ab167453), anti-Rabbit IgG-HRP (ab6721), and anti-FLAG-Rabbit IgG (ab1162) were purchased from Abcam (Cambridge, UK). 4-(4,6-dimethoxy-1,3,5-triazin-2-yl)-4-methylmorpholinium chloride

(DMTMM), DBCO-COOH, Tween-20 and 3,3′,5,5′-tetramethylbenzidine were purchased from Sigma-Aldrich (Massachusetts, US). Varioskan microplate reader, Nanodrop 2000, Alexa Fluor 647 NHS ester, and fetal bovine serum (FBS) were purchased from Thermo Fisher Scientific (Massachusetts, US). N-(4-pentynoyl)-mannosamine-tetraacylated (Ac_4ManNAlk) was purchased from Click Chemistry Tools (AZ, USA). HeLa was purchased from Anti-Cancer Japan (Chiba, Japan).

Method

Preparation of DBCO-Coated Glass (DBCO Glass)

The φ13 mm glass slides were initially cleansed in an alkaline solution composed of NH_3:H_2O_2: H_2O in a 1:1:5 (v/v) ratio. The glass slides were then reacted at room temperature for 2 h in piranha solution (H_2SO_4: H_2O_2 = 4:1 (v/v)). Following this, the glass slides were reacted at room temperature for 24 h in a silane solution (MPTMS: EtOH: dH_2O = 1:95:4 (v/v)), and subsequently heated at 110 ℃ for 1 h. The heated glass slides were then reacted at room temperature for 24 in a solution of Maleimide-PEG-NH_2 and Maleimide-PEG-Methyl in a 7:3 (w/w) ratio, dissolved in D-PBS(-) at a concentration of 2 mg/mL Finally, the slides were immersed in a reagent solution dissolved in D-PBS(-) containing DBCO-COOH and DMTMM at concentrations of 1.2 mM and 3 mM, respectively, to coat the glass with DBCO. The presence of DBCO groups on the glass surface was evaluated by reacting with Texas-RED-PEG_3-Azide at a concentration of 10 μM for 15 min and observing the fluorescence.

Expression and Purification of Anti-mCherry VHH-AzF-HN and Anti-EmGFP VHH-AzF-HN

Escherichia coli BL21(DE3) was co-transformed with plasmids encoding Anti-mCherry VHH-AzF and Anti-EmGFP VHH-AzF, along with the pCDF/pAzAz plasmid, which includes genes for UAG-reading tRNA, based on a previously reported method [59]. The structures of anti-mCherry VHH and anti-EmGFP VHH were sourced from the Protein Data Bank [60,61]. VHHs are expressed with a 6 × histidine and asparagine (HN) affinity tag to obtain Anti-mCherry VHH-AzF-HN and Anti-EmGFP VHH-AzF-HN. The *Escherichia coli* cultures, grown in LB medium, were incubated at 23 °C until an OD600 of about 0.6 was reached. Expression was then induced by adding 1.0 mM Isopropyl-β-d-thiogalactopyranoside (IPTG) and H-Phe(4-N_3)-OH (AzF), followed by continued incubation at 23 °C and 180 rpm for 48 h. The cultures were subsequently lysed using high-pressure homogenization, and the lysate was centrifuged at 12000 × g for 15 min to separate the soluble and insoluble fractions. The soluble fraction underwent purification using TALON metal affinity resin to extract HN-tagged proteins, which were then transferred into a 50 mM Arginine Hydrochloride, 10 mM HEPES, 130 mM Sucrose buffer (Arg·HCl/HEPES/Sucrose buffer) using an Amicon ultra 15, 10 kDa MWCO. The VHH concentration was quantified by measuring the absorbance at 280 nm. To verify the activity of the introduced azide groups in VHH, DBCO-PEG_4-5/6-FAM was added to each sample and incubated at

37 °C for 30 min. The samples were analyzed by SDS-PAGE, and images were captured to document both FAM-derived fluorescence and CBB staining.

Expression and Purification of mKO2 and mKO2-AzF

Escherichia coli BL21(DE3) was co-transformed with plasmids encoding mKO2 and mKO2-AzF, along with the pCDF/pAzAz plasmid. The cultures were grown until an OD600 of approximately 0.6 at 23 ℃. Subsequently, IPTG was added to a final concentration of 1 mM to induce expression in *Escherichia coli* harboring mKO2 plasmids. For cultures expressing mKO2-AzF, 1 mM IPTG and H-Phe(4-N_3)-OH were added. The cultures were further incubated for 48 h at 15 ℃. The *Escherichia coli* cells were then suspended in D-PBS(-), lysed using a high-pressure homogenizer, and the soluble fraction obtained was affinity-purified using Ni Sepharose 6 Fast Flow, followed by buffer exchange into D-PBS(-). The concentrations of mKO2, and mKO2-AzF were determined by measuring the absorbance at 280 nm using Nanodrop 2000.

Expression and Purification of GST-tagged mCherry/EmGFP

Escherichia coli BL21(DE3) was transformed with Glutathione S-transferase (GST) tagged mCherry/EmGFP expression plasmids and cultured at 23 °C. The growth of these cultures was monitored until the optical density at 600 nm (OD600) reached about 0.6. Following this, the expression of GST-tagged mCherry and EmGFP proteins was initiated by adding IPTG to a concentration of 1 mM. The cultures were then incubated for 48 h at 15 °C to facilitate protein expression. Post incubation, the bacterial cells were suspended in D-PBS(-) and lysed using a high-pressure homogenizer to release the cellular contents. The soluble fractions from the lysate were then isolated and subjected to affinity purification using COSMOGEL GST-Accept, specifically targeting the GST-tagged mCherry and EmGFP proteins. After the purification process, the protein solutions were buffer-exchanged into D-PBS(-) to finalize the preparation of the purified proteins.

Antigen Binding Evaluation of Anti-mCherry VHH-AzF-HN and Anti-EmGFP VHH-AzF-HN

COSMOGEL GST-Accept was substituted with D-PBS(-). 30 μL of COSMOGEL GST-Accept was added to a 200 μL tube, and the solution was removed by centrifugation. Next, 30 μL of either 10 μM GST-mCherry in D-PBS(-), 10 μM GST-EmGFP in D-PBS(-), or D-PBS(-) was added, and the mixture was shaken at 800 rpm at room temperature for 30 min. The supernatant was removed by centrifugation, and the precipitate was incubated with 30 μL of 10 μM Anti mCherry VHH(AzF) or Anti EmGFP VHH(AzF) in D-PBS(-) at 4 ℃, 500 rpm for 30 min. The mixture was then centrifuged at 12000 × g for 1 min using Ultrafree-MC, HV, 0.45 μm for filtration and resin removal (Flowthrough fraction). An additional 30 μL of D-PBS(-) was added, followed by further centrifugation at 12000 × g. To the resin, 30 μL of 100 mM glutathione solution was added and centrifuged at 12000 × g for 1 min (Elution

fraction). SDS-PAGE was performed on each fraction, and CBB staining images were captured.

Transfection of tANCHOR-mCherry Expression Plasmid and Generation of Stable Cell Lines (mCherry coated cell)

The tANCHOR system [62] is an effective tool to display mCherry on the outer membrane of cells. The tANCHOR-mCherry plasmid was cloned into the Piggy Bac Transposon vector system PB533A-2, which is G418 resistant. HeLa cells were plated at a density of 1×10^4 cells per well in a 96-well plate. When the cells reached 80% confluency, they were transfected. The transfection mixture for each well comprised 0.6 μL of FuGENE 6, 0.1 μg of the tANCHOR-mCherry plasmid, and the transposase vector. This mixture was prepared in a total volume of 5 μL using Opti-MEM Reduced Serum Medium and subsequently added to the cells. After 48 h of transfection, cells were selected for resistance using DMEM containing 10% FBS, 1% Penicillin-Streptomycin-Glutamine (PSG), and 0.8 mg/mL of the antibiotic G418. Within five days, non-transfected HeLa cells perished, allowing for the isolation of colonies using the limiting dilution method. Cells were then plated at one cell per well in a 96-well plate. The medium was refreshed every alternate day until the cells reached 80% confluence. The cells were then progressively scaled up through various plate sizes: from 48-well to 24-well, 12-well, and finally 6-well plates. The mCherry fluorescence in these cells was observed under an OLYMPUS IX73 microscope.

Detection of Membrane Surface mCherry in Stable Cell Lines

The mCherry coated cells were initially plated at a density of 2.0×10^4 cells per well in a 96-well plate and cultured for 24 h. For fixation, the cells were treated with 4% paraformaldehyde at 15 °C for 10 min and then washed twice with 300 mL of D-PBS(-). To block non-specific binding, the cells were incubated for 2 h with 200 μL of blocking buffer, which consisted of D-PBS(-) containing 3% bovine serum albumin. Following the blocking step, 100 μL of diluted primary antibodies were added to the cells. These antibodies included anti-mCherry-Rabbit IgG and anti-FLAG-Rabbit IgG, each at a concentration of 1 mg/mL in blocking buffer. The cells were incubated with these antibodies for 2 h and then washed three times with 300 μL of D-PBS(-) with 0.05% Tween-20 (v/v). The next step involved a 2-hour incubation with 100 μL of diluted secondary antibody, specifically anti-Rabbit IgG-HRP at 0.1 mg/mL in blocking buffer. After this, the cells were washed five times with 300 μL of D-PBS(-) with 0.05% Tween-20. For detection, each well was incubated with 100 μL of TMB (3,3′,5,5′-tetramethylbenzidine) substrate at room temperature for 30 min. This was followed by the addition of 100 μL of stop solution (2 M HCl). Finally, the absorbance at 450 nm for each well was measured using a Varioskan microplate reader.

Evaluation of the Functional Group-Specific Binding of Azide-Introduced Proteins to DBCO Glass

The mKO2 and mKO2-AzF were each adjusted to a concentration of 10 μM and added to DBCO glass and methyl-coated glass. The mixtures were then incubated at 37 ℃ for 1 h. Following the incubation, the glasses were washed twice with D-PBS(-) and then evaluated by fluorescence observation.

Evaluation of Antigen-Binding Capacity of VHH Immobilized on DBCO Glass

Anti mCherry VHH(AzF) and anti EmGFP VHH(AzF), each at a concentration of 10 μM, were dropwise added at 0.1 μL onto DBCO glass and incubated at 37 ℃ in a humid environment for 1 h. The glass was subsequently washed twice with D-PBS(-), followed by a 30 min reaction in D-PBS(-) with 3% BSA. After two additional washes with D-PBS(-) containing 1% BSA, the glass was reacted with a mixed solution of 10 μM mCherry and EmGFP, or mCherry alone, EmGFP alone, or D-PBS(-) with 1% BSA, followed by two washes with D-PBS(-) containing 0.1% BSA. The bound mCherry or EmGFP was determined by fluorescence observation.

Evaluation of Adhesion of mCherry coated Cell to VHH-conjugated glasses

After anti mCherry VHH(AzF) coated on DBCO glasses, mCherry-coated cells or normal HeLa cells labeled with Calcein-AM were detached using Accutase and suspended in DMEM. Subsequently, 500 μL of the cell suspension was seeded onto the VHH-binding substrate and incubated at 37 ℃ in 5% CO_2 for 1 h. To prevent non-specific adhesion, the culture medium was replaced with 0.5 mL EDTA cell dissociation buffer in enzyme-free Hanks' balanced salt solution, followed by incubation at room temperature for 5 min. Subsequently, the glasses were washed twice with 1 mL of D-PBS(-).

Evaluation of Antigen-Antibody Dependent Cell Adhesion

The anti mCherry VHH conjugated substrate was preincubated with DMEM (10% FBS), 1 μM mCherry in DMEM (10% FBS), or 1 μM EmGFP in DMEM (10% FBS). Then, mCherry coated cells or HeLa cells, with Calcein-am labeling were added at a concentration of 7.5×10^5 cells/mL. The cells were incubated at 37℃ in a 5% CO_2 environment for 1 h. Afterwards, the cells were permeabilized at room temperature at 300 rpm for 3 min using an Eppendorf Thermo Mixer C, followed by two washes with D-PBS(-). The fluorescence intensity of the cell lysates, dissolved in 0.25% Triton X-100 in D-PBS(-), was measured using a Thermo Fisher Scientific Varioskan.

1.3 Result

1.3.1 Binding of mKO2-AzF to DBCO-coated glass

When Texas-RED-PEG_3-Azide was reacted with DBCO-coated glass, fluorescent signals were detected on the glass surface (Fig. 1a). In contrast, a little fluorescence was observed when Texas-RED-PEG_3-Azide was reacted with methyl-coated glass, confirming the presence of DBCO coating on the glass. As a model protein for binding to the DBCO-coated glass, azidophenylalanine was introduced into the fluorescent protein mKO2. SDS-PAGE analysis revealed a protein with a molecular mass of 30 kDa. Further, the reaction of the obtained protein with DBCO-PEG_4-5/6-FAM confirmed its reactivity with the azide group (Fig. 1b). Both mKO2-AzF and mKO2 were added to either DBCO-coated or methyl-coated glass and reacted. Fluorescence signals from mKO2 were detected only in the group where mKO2-AzF was reacted with DBCO-coated glass (Fig. 1c).

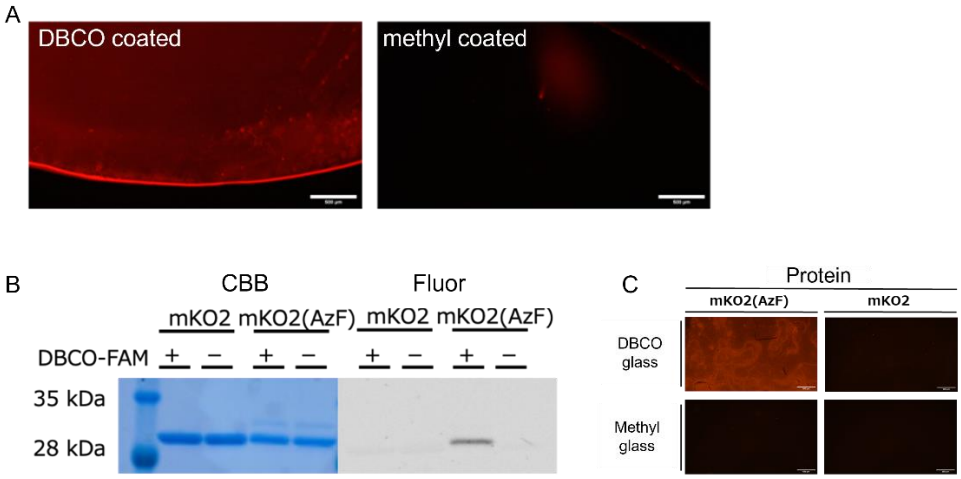

Fig. 1. Evaluation of protein binding and fluorescence observation on DBCO and methyl-coated glass surfaces

a) Fluorescence observation was performed after reacting Texas-Red-Azide with glass coated with DBCO and methyl groups. The observations were made using an OLYMPUS IX73 microscope with a red filter (EX; 530-550 nm, DM; 570 nm, EM; 575 nm) b) After reacting mKO2 or mKO2-AzF with DBCO-FAM, the samples were analyzed by SDS-PAGE. The images show the gel after CBB staining and the fluorescent images captured before CBB staining. c) Fluorescence observation was conducted after reacting mKO2-AzF or mKO2 with glass coated with either DBCO or methyl groups. The observations were performed using an OLYMPUS IX73 microscope with a red filter. Scale bar = 500 μm.

1.3.2 Expression of anti mCherry VHH(AzF) and anti EmGFP VHH(AzF)

Azido-phenylalanine was inserted into anti mCherry VHH and anti EmGFP VHH. SDS-PAGE analysis showed that both anti mCherry VHH(AzF) and anti EmGFP VHH(AzF) had a molecular mass

of approximately 16 kDa. Additionally, the reaction of both VHHs with DBCO-PEG$_4$-5/6-FAM indicated their reactivity with the azide group (Fig. 2a). Subsequently, the antigen-binding ability of each VHH was evaluated. Solutions containing glutathione S-transferase (GST)-tagged mCherry or EmGFP, or without them, were added to glutathione agarose resin, followed by the addition of anti mCherry VHH or anti EmGFP VHH. The unbound fractions (Flowthrough) and the glutathione eluted fractions (Elution) were analyzed by SDS-PAGE (Fig. 2b). Bands near 55 kDa were identified as mCherry or EmGFP, and bands near 16 kDa were identified as anti mCherry VHH or anti EmGFP VHH. In the lanes with blank resin, VHH bands were observed in the unbound fractions but not in the eluted fractions. It was confirmed that anti mCherry VHH or anti EmGFP VHH hardly bound to the resin. Anti mCherry VHH was observed in the eluted fraction of mCherry-bound resin and in the unbound fraction of EmGFP-bound resin, indicating antigen-selective binding. A similar result was obtained for anti EmGFP VHH.

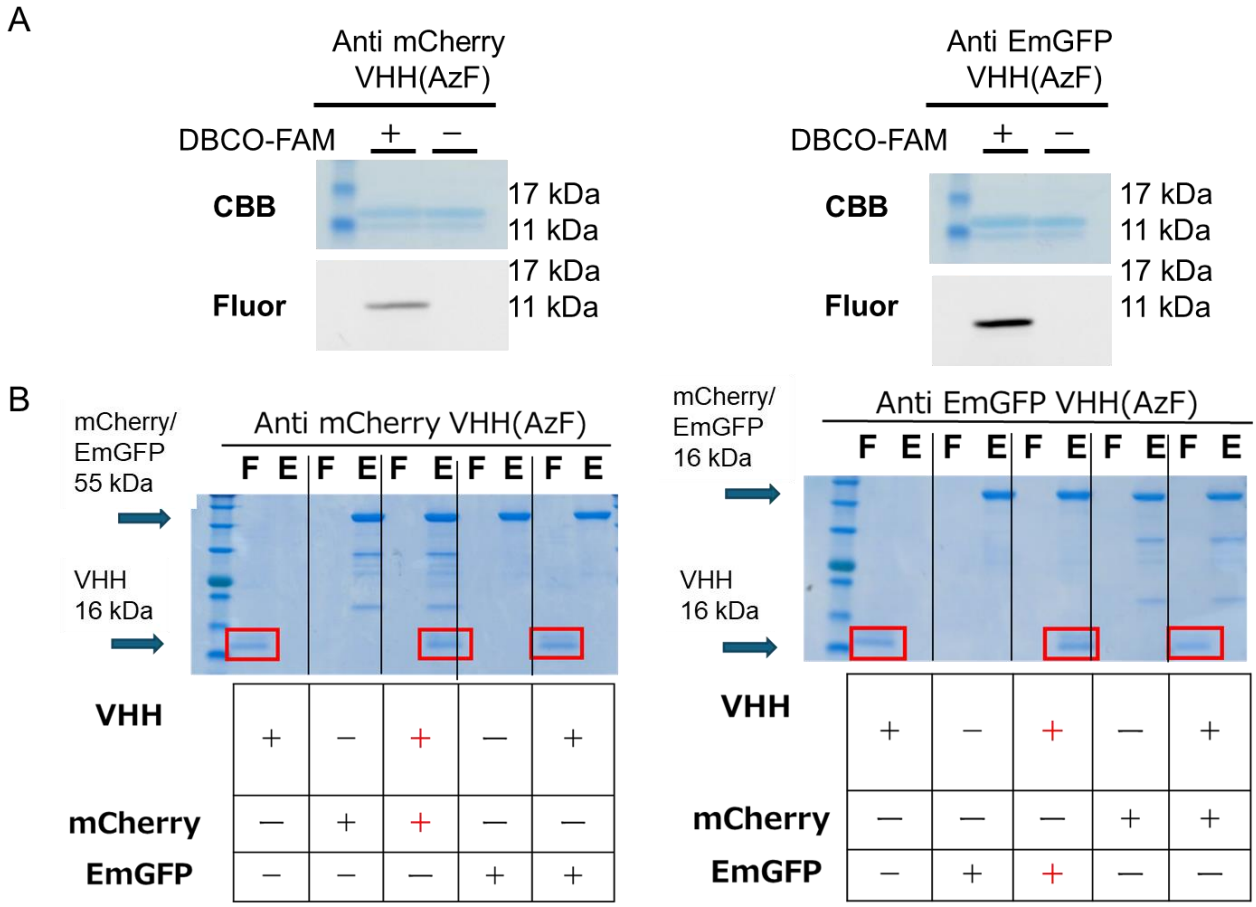

Fig. 2. Characterization and evaluation of azide activity and binding affinity of anti mCherry VHH(AzF) and anti EmGFP VHH(AzF)

a) After reacting anti mCherry VHH(AzF) or anti EmGFP VHH(AzF) with DBCO-FAM, the samples were analyzed by SDS-PAGE. The figure shows the gel after CBB staining and the fluorescent images captured before CBB staining. b) Anti mCherry VHH(AzF) or anti EmGFP VHH(AzF) were added to resin bound with mCherry or EmGFP via a GST-tag. The unbound fractions (F=Flow through) and the bound fractions (E=Elution), obtained by adding 100 mM glutathione, were analyzed by SDS-PAGE,

and the gels were stained with CBB.

1.3.3 Selective binding of mCherry and EmGFP on glass coated with two types of VHHs

After sequentially dropping and binding anti mCherry VHH(AzF) and anti EmGFP VHH(AzF) on a single piece of DBCO glass, a mixed solution of mCherry and EmGFP, or solutions containing only mCherry or only EmGFP were reacted. In each group, fluorescent signals of mCherry or EmGFP were observed at the positions corresponding to the respective antibodies (Fig. 3).

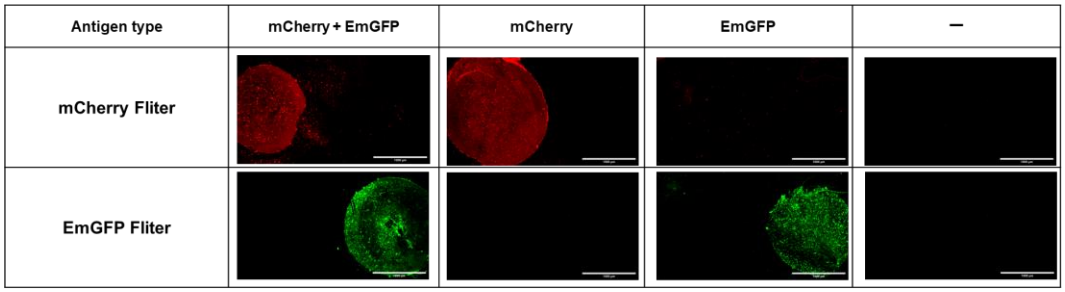

Fig. 3. Evaluation of antigen recognition ability of VHHs immobilized on a substrate

Anti mCherry VHH(AzF) (on the left side of the glass) and anti EmGFP VHH(AzF) (on the right side of the glass) were sequentially dropped and reacted with a mixed solution of mCherry and EmGFP, a solution of mCherry, a solution of EmGFP, and D-PBS(-) containing 1% BSA. The samples were then observed by fluorescence microscopy. Imaging was performed using an Olympus IX73 microscope (for mCherry: Red filter (EX; 530-550 nm, DM; 570 nm, EM; 575 nm), and for EmGFP: Green filter (EX; 470-495 nm, DM; 505 nm, EM; 510-550 nm). Scale bar = 1 mm.

1.3.4 Establishment of mCherry-coated HeLa cell line

A cell line expressing mCherry on the cell membrane was established using the tANCHOR system. The intracellular expression of the FLAG tag and the membrane expression of mCherry were utilized to evaluate the cell line with a cell-based assay, using anti-FLAG (control) and anti-mCherry (treatment) antibodies as primary antibodies, and anti-Rabbit IgG (HRP conjugate) as the secondary antibody (Fig. 4). The cells treated with anti-mCherry antibody showed the highest activity, and significantly higher HRP activity was observed compared to cells treated with anti-FLAG antibody. These results suggest that mCherry is expressed extracellularly.

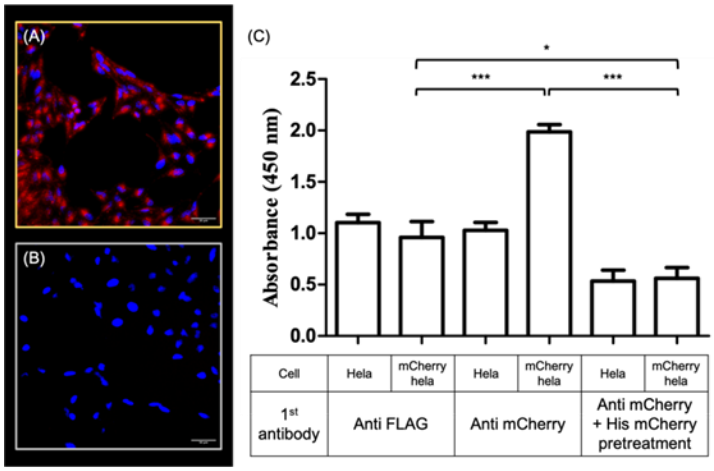

Fig. 4. Establishment and analysis of mCherry-coated HeLa cell line using tANCHOR

A HeLa cell line expressing mCherry on the cell membrane was successfully established utilizing the tANCHOR system. Fluorescence microscopy images of the mCherry-coated HeLa cells (A) and regular HeLa cells (B) were captured (OLYMPUS IX73) and showed Texas Red (red) and DAPI (blue) staining. Scale bar = 100 μm. C) Both cell types were seeded and cultured for 24 h, followed by fixation with 2% formaldehyde. Primary antibodies targeting either FLAG tags or mCherry were added to the cells, then reacted with HRP-conjugated secondary antibodies. Subsequently, HRP activity was measured at an absorbance of 450 nm. As a control, a group where the primary antibody against mCherry was reacted with an excess amount of mCherry was prepared. Each result represents the mean ± S.D and is performed in Tukey's test. *** $p < 0.001$, * $p < 0.05$.

1.3.5 Selective adhesion of mCherry coated cell to anti mCherry VHH conjugated glass

HeLa cells and mCherry coated cells were seeded onto an anti mCherry VHH conjugated glass. During a reaction time of up to 1.5 h, the number of adhered cells increased with time (Fig. 5a). The number of adhered mCherry-HeLa cells was significantly higher than that of HeLa cells (Fig. 5b). Regarding the reaction concentration, the number of adhered mCherry-HeLa cells increased with concentration up to 1×10^6 cells/mL, but showed little increase thereafter (Fig. 5c). At all concentrations, the number of adhered mCherry-HeLa cells was significantly higher than that of HeLa cells.

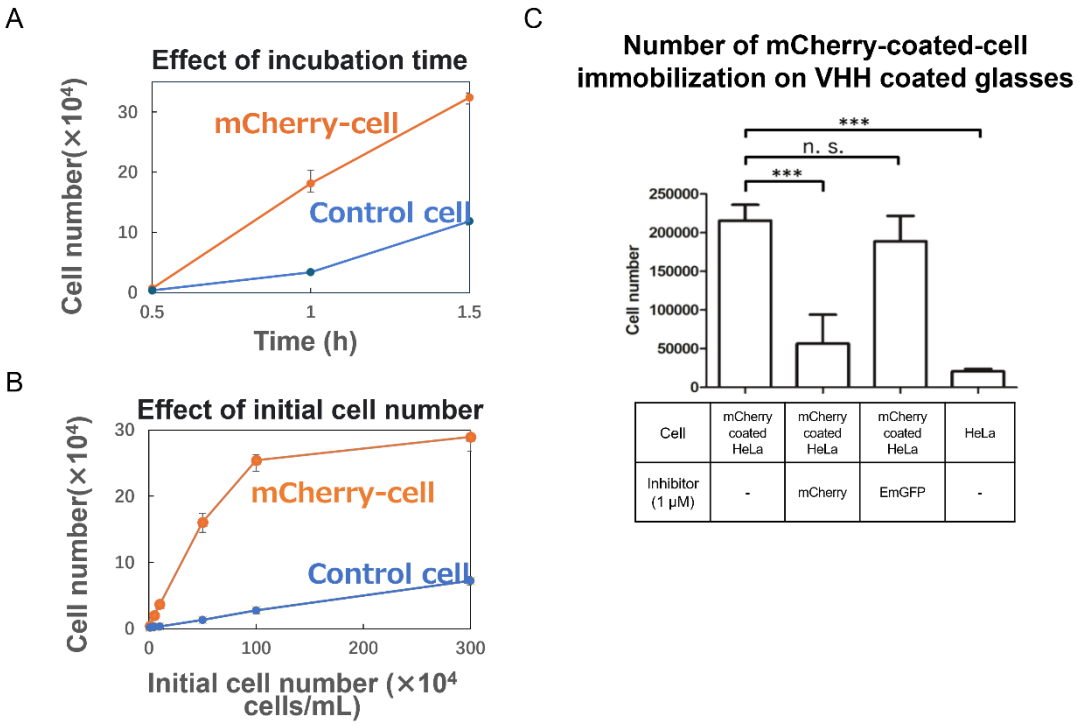

Fig. 5. Analysis of selective cell adhesion and antigen-antibody interaction on anti mCherry VHH conjugated glasses

a) HeLa cells or mCherry-HeLa cells, labeled with CalceinAM, were added to an anti mCherry VHH conjugated glass at a concentration of 7.5×10^5 cells/mL and in a volume of 500 μL. The reaction was conducted for 0.5, 1, and 1.5 h. b) HeLa cells or mCherry coated cells, labeled with Calcein-AM, were added to the anti mCherry VHH conjugated glass at various concentrations (1×10^4, 5×10^4, 1×10^5, 5×10^5, 1×10^6, 3×10^6 cells/mL) in a volume of 500 μL and reacted for 60 min. In both cases, the reactions were carried out at 37 ℃ under 5% CO_2, followed by permeabilization at room temperature at 300 rpm for 3 min and two washes with D-PBS(-). The fluorescence intensity of the cell lysates, dissolved in 0.25% Triton X-100 in D-PBS(-), was measured using a Thermo Fisher Scientific Varioskan and cell numbers were calculated from a standard curve (Em; 490 nm, Ex; 515 nm, n=3). c) After preincubating the anti mCherry VHH conjugated glass with DMEM (10% FBS), 1 μM mCherry in DMEM (10% FBS), or 1 μM EmGFP in DMEM (10% FBS), mCherry coated cells or HeLa cells were added at a concentration of 7.5×10^5 cells/mL. The reaction was conducted for 1 h at 37 ℃ under 5% CO_2, followed by permeabilization at room temperature at 300 rpm for 3 min and two washes with D-PBS(-). The fluorescence intensity of the cell lysates, dissolved in 0.25% Triton X-100 in D-PBS(-), was measured using a Thermo Fisher Scientific Varioskan and cell numbers were calculated from the standard curve. Data for all groups are presented as mean ± standard deviation. Multiple comparisons between groups were performed using Tukey's method. *** $p < 0.001$, n=3.

1.4 Discussion

The incorporation of AzF into VHH is an innovative approach that maintains both azide reactivity and antigen binding affinity. This is substantiated by the experiment where mKO2-AzF, compared to its non-AzF counterpart, successfully adhered to DBCO glasses, demonstrating the retention of azide functionality post-incorporation (Fig. 1). This observation aligns with the findings of Wang et al., who reported the successful immobilization of lipase-AzF on DBCO-coated well-plates, confirmed through Fourier-transform infrared spectroscopy. Further evidence of the maintained binding affinity of VHH-AzF is provided where mCherry and EmGFP were selectively captured on their respective VHH-antibody coated areas (Fig. 4). Additionally, mCherry-labeled HeLa cells were specifically immobilized on surfaces coated with mCherry-VHH, unlike untagged HeLa cells. This specificity underlines the preserved antigen-binding affinity of VHH-AzF post-fixation. A similar outcome was observed in Trilling's work [63], where VHH A23-AzF effectively captured heat-shock proteins. In summary, the incorporation of AzF into VHH is a powerful technique for the site-specific conjugation of antibodies on substrates, offering significant potential for biochemical applications.

The application of cell immobilization using aligned VHH-AzF is highlighted. The selective capture of mCherry and EmGFP on corresponding VHH-antibody coated areas (Fig. 2), and the immobilization of mCherry-labeled HeLa cells (Fig. 4), emphasize the binding specificity of aligned VHH-AzF. Trilling et al. [63] expanded this concept by immobilizing anti-peptide PAT49 VHH-AzF on a well-plate, which successfully captured the foot-and-mouth disease virus, demonstrating the capacity of immobilized and aligned VHH to capture viruses or cells. This technique represents an advancement over previous methods that used independent pairs for cell immobilization. Limitations such as the restricted range of click pairs and challenges in cell labeling were significant hindrances. By switching to antigen-antibody pairs, which target cells' endogenous antigens, the process becomes more versatile and accessible, potentially paving the way for broader applications in various fields.

Alignment plays a crucial role in enhancing binding affinity, as illustrated in protein and cell capture applications. Balevicius et al. [64] demonstrated that oriented antibodies can bind analytes 2.5 times more efficiently than randomly immobilized antibodies. Similarly, Chen et al. [65] found that the efficiency of cell-capturing, particularly of endothelial progenitor cells (EPC) using anti-CD34 antibodies, was significantly higher with oriented immobilization compared to random fixation, under flow conditions. However, VHH lacks an Fc region, necessitating an alternative method for alignment. Trilling et al. [66] showed that anti-peptide PAT49 VHH-AzF, when aligned on a surface plasmon resonance (SPR) sensor via click reaction, exhibited an 800-fold higher affinity compared to randomly fixed antibodies. My method, which facilitates the aligned immobilization of VHH-AzF, is advantageous for applications such as cell-based ELISA and can yield more precise results. The ability

to orient antibodies precisely not only enhances their binding capacity but also increases the efficiency and specificity of the immobilization process, which is crucial for sensitive and accurate biochemical assays.

Section 2. Effect of peptide spacer between VHH antibody and cell membrane on programmed cell-cell interaction

2.1 Introduction

Cell-cell interactions play a vital role in the burgeoning field of cell-based therapies, which are gaining promise in treating a wide variety of disease states. These therapies include applications in mesenchymal stem cells (MSCs) for neurodegenerative diseases [67], cardiovascular diseases [68], and the rapidly evolving domain of CAR-T cell immunotherapy [69]. The success of these therapies heavily relies on the precise control and manipulation of cell-cell interactions, which are fundamental to their therapeutic efficacy. However, achieving controlled and productive cell-therapy outcomes presents significant challenges. For instance, studies involving systemic injections of MSCs in rat models of myocardial infarction have shown that less than 1% of the injected MSCs accumulate in the ischemic myocardium [70]. This low efficacy rate highlights the necessity for enhanced targeting and interaction of therapeutic cells with specific tissues. In contrast, when MSCs are induced to upregulate the CXCR4 receptor prior to infusion, there is more than a two-fold increase in the homing of these cells to ischemic tissues [71]. This example underscores the importance of modulating cell-cell interactions to improve the targeting and effectiveness of cell-based therapies. Therefore, the ability to regulate cell-cell interactions is not only crucial for advancing fundamental chemical biology studies but also holds immense promise for the development of more effective therapeutic strategies. Understanding and manipulating these interactions can lead to significant improvements in the delivery and efficacy of cell-based therapies, opening new avenues in the treatment of complex diseases.

Genetic engineering, exemplified by CAR-T cell therapy, has become the preeminent method in clinical cellular engineering. CAR-T cells, engineered to express cancer-recognizing proteins on their surface, effectively mediate interactions with cancer cells [72]. Similarly, overexpressing CXCR4 on MSCs enhances their capacity for recognizing and chemotaxing toward stromal-derived factor-1 (SDF-1) [73]. Despite these successes, genetic engineering is often time-consuming, inefficient, and carries the burden of permanent and irreversible modifications [73]. These alterations can lead to significant adverse events in patients, raising safety concerns for long-term clinical use [74]. In response to these challenges, non-genetic cell-surface modifications have emerged as a promising alternative, particularly in modulating cell-cell interactions through protein-protein interactions within cellular membranes. These strategies include lipid-protein insertion onto the cell surface [75], conjugation of biotinylated cells with streptavidin-tagged proteins [76], metabolic labeling of cells with complementary click ligand-tagged proteins [77], and conjugation of proteins to N-terminal glycine residues using "sortagging" enzymes [78]. These methods offer the potential to replace genetic approaches in certain contexts, especially where

the risks associated with genetic modification are too great. In the realm of chemical modifications, the design of protein ligands is critical. My previous work using click chemistry [79] highlighted the importance of alignment and spacer design. Maintaining the binding affinity of the modified protein is crucial, as modifications like biotin-streptavidin may interfere with the protein's binding site [74]. Additionally, the main purpose of the spacer is to enhance the yield of cell-protein conjugation. For instance, cell membrane modification with different PEG lengths of DOPE-PEG-benzylguanine showed that only those with more than 17 PEG groups were capable of binding to DNA methyltransferase (SNAP-tag) through a benzylguanine-thiol bond [80].

The design of the spacer in CAR-T therapy plays a crucial role, impacting both the function and efficacy of the therapeutic cells. Primarily derived from natural T cell receptors (TCR), spacers have a significant influence on the expression levels and stability of the chimeric antigen receptor (CAR). This, in turn, promotes prolonged presence of CAR on the cell surface, enhancing the expansion and persistence of T cells in the therapeutic context [81,82]. Moreover, the presence and design of the spacer are critical for effective cell-cell interactions. For instance, in studies involving single-chain-variable fragment (scFv)-zeta chimeras, only those containing a spacer region exhibited ErbB-2 binding activity when expressed in T cells [83]. This finding underscores the importance of structural elements in the spacer region for functional antigen recognition and binding. Furthermore, a comparison of spacers of varying lengths revealed that only a long spacer (220 amino acids) was effective in eliminating tumor cells, as opposed to designs with a very short spacer (12 amino acids) [84]. Meanwhile reducing the flexibility of spacer also impedes CD19 CAR-T cell's therapy efficacy [85]. These highlight the crucial role of spacer in mediating effective cell-cell interactions and therapeutic outcomes. In chemical modification, I also think spacer characteristics like length or flexibility may affect cell-cell interaction.

In this study, my aim was to investigate the role of fusion peptide spacers in enhancing cell-cell interaction. To this end, I created variable domain of heavy chain of heavy-chain (VHH) constructs incorporating two different peptide spacers: a flexible spacer consisting of a triple-repeat glycine-serine sequence (GGGGS) and a more rigid spacer with a triple-repeat glutamic acid-alanine-lysine sequence (EAAAK). My focus was on examining how the flexibility of these spacers affects cell-cell interactions. My approach involved the use of an anti-mCherry VHH, incorporated with azido-phenylalanine (AzF), to facilitate selective cell adhesion. This was achieved by first introducing an alkyne group into GFP-HeLa cells, which allowed for the subsequent connection of these cells to the VHH via a click reaction. I then developed a system involving HeLa cells expressing mCherry on their surface (referred to as mCherry-coated cells) and harvested them onto plates to create a primary cell layer. Both VHH-conjugated and unmodified GFP-HeLa cells were incubated over this mCherry-coated layer. My results indicated that a significantly higher number of VHH-modified cells remained adhered to the mCherry-coated cells compared to the unmodified cells. Furthering my investigation, I incorporated peptide spacers between the VHH and AzF. Remarkably, these peptide spacers further enhanced cell adhesion to

the mCherry-coated first cell layer. My findings suggest that VHH equipped with a peptide spacer can be a valuable tool for cell immobilization to targeted cells, opening new avenues for cell-based therapies and interactions.

2.2 Materials and methods

Materials

Escherichia coli BL21(DE3) was purchased from BioDynamics Laboratory, Inc. (Tokyo, Japan). Arginine Hydrochloride (Arg·HCl), Accutase, COSMOGEL GST-Accept, Hydrogen chloride, LB medium, 4-(2-hydroxyethyl)-1-piperazineethanesulfonic acid (HEPES), Dulbecco's Modified Eagle Medium (DMEM), Penicillin-Streptomycin-Glutamine (PSG), Sucrose, paraformaldehyde, Isopropyl-β-d-thiogalactopyranoside (IPTG), and trypsin were purchased from Nacalai Tesque (Kyoto, Japan). H-Phe(4-N_3)-OH(AzF) was purchased from Watanabe Chemical Industries, Ltd. (Hiroshima, Japan). High-pressure homogenizer (EmulsiFlex-B15) was purchased from AVESTIN (Ottawa, Canada). TALON metal affinity resin was purchased from Takara Bio (Shiga, Japan). 48-well, 24-well, 12-well, and 6-well plates were purchased from Corning (NY, USA). Ultrafree -MC, HV, 0.45 μm and Amicon ultra 15, 10 kDa MWCO were purchased from Millipore Co. (Massachusetts, US). DBCO-PEG_4-5/6-FAM and 5/6-Texas Red-PEG_3-Azide were purchased from Jena BioScience (Jena, Germany). D-PBS(-) was purchased from Nissui (Tokyo, Japan). Ni Sepharose 6 Fast Flow was purchased from Cytiva (Massachusetts, US). 96-well plate Greiner was purchased from Bio-One (Kremsmuenster, Austria). FuGENE 6 was purchased from Promega (Wisconsin, US). Opti-MEM Reduced Serum Medium was purchased from Gibco (Massachusetts, US). Anti-mCherry-Rabbit IgG (ab167453), anti-Rabbit IgG-HRP (ab6721), and anti-FLAG-Rabbit IgG (ab1162) were purchased from Abcam (Cambridge, UK). 4-(4,6-dimethoxy-1,3,5-triazin-2-yl)-4-methylmorpholinium chloride (DMTMM), DBCO-COOH, Tween-20 and 3,3′,5,5′-tetramethylbenzidine were purchased from Sigma-Aldrich (Massachusetts, US). Varioskan microplate reader, Nanodrop 2000, Alexa Fluor 647 NHS ester, and fetal bovine serum (FBS) were purchased from Thermo Fisher Scientific (Massachusetts, US). N-(4-pentynoyl)-mannosamine-tetraacylated (Ac_4ManNAlk) and 2-(4-((bis((1-(tert-butyl)-1H-1,2,3-triazol-4-yl)methyl)amino)methyl)-1H-1,2,3-triazol-1-yl)acetic acid (BTTAA) were purchased from Click Chemistry Tools (AZ, USA). HeLa and green fluorescent protein-HeLa (GFP-HeLa) were purchased from Anti-Cancer Japan (Chiba, Japan).

Methods

Expression and Purification of Anti-mCherry VHH-AzF-HN / Anti-mCherry VHH-$(GGGGS)_3$-AzF-HN / Anti-mCherry VHH-$(EAAAK)_3$-AzF-HN

The pCDF/pAzAz plasmid, carrying genes for UAG-reading tRNA was based on the previous report [59]. The sequence and structure of anti-mCherry VHH was from protein data bank [60]. Plasmids of Anti-mCherry VHH-AzF-HN (hereafter referred to as VHH), Anti-mCherry VHH-$(GGGGS)_3$-AzF-HN (VHH-$(GGGGS)_3$), and Anti-mCherry VHH-$(EAAAK)_3$-AzF-HN (VHH-$(EAAAK)_3$) along with pCDF/pAzAz_were co-transformed into *Escherichia coli* BL21(DE3). VHHs are expressed with a 6 × histidine and asparagine (HN) affinity tag to obtain Anti-mCherry VHH-AzF-HN, Anti-mCherry VHH-$(GGGGS)_3$-AzF-HN, and Anti-mCherry VHH-$(EAAAK)_3$-AzF-HN. The cultures were grown in LB medium at 23 °C with shaking until OD600 reached approximately 0.6. Subsequently, expression was induced by adding IPTG and H-Phe(4-N_3)-OH(AzF) to a final concentration of 1.0 mM, followed by further incubation at 23 °C and 180 rpm for 48 h. The resulting culture was lysed using a high-pressure homogenizer, and the lysate was centrifuged at 12000 × g for 15 min. The pellet was collected as the insoluble fraction, and the supernatant as the soluble fraction. The soluble fraction was purified using TALON metal affinity resin to isolate the HN-tagged proteins, which were subsequently buffer-exchanged into 50 mM Arginine Hydrochloride/10 mM HEPES/130 mM Sucrose buffer (Arg·HCl /HEPES/Sucrose buffer) using Amicon ultra 15, 10 kDa MWCO. The concentration of VHH was determined by measuring absorbance at 280 nm. To assess the activity of the azide groups introduced into VHH, DBCO-PEG_4-5/6-FAM was added to each sample, incubated at 37 °C for 30 min, followed by SDS-PAGE analysis. Images were captured for both FAM-derived fluorescence and CBB staining.

Expression and Purification of His-tagged mCherry and GST-tagged mCherry/EmGFP

Escherichia coli BL21(DE3) strains, transformed with His-mCherry and GST-mCherry/EmGFP expression plasmids, were cultured at 23 °C until the OD600 reached approximately 0.6. Expression of both proteins was induced by adding IPTG to a final concentration of 1 mM, followed by an incubation period of 48 h at 15 °C. The bacteria were subsequently suspended in D-PBS(-) and lysed using a high-pressure homogenizer. The soluble fractions obtained were processed for affinity purification: the His-tagged mCherry using Ni Sepharose 6 Fast Flow and the GST-tagged mCherry/EmGFP using COSMOGEL GST-Accept. Following purification, the buffers for both proteins were exchanged with D-PBS(-) to complete the process.

Antigen Binding Evaluation of Anti-mCherry VHH-AzF-HN / Anti-mCherry VHH-$(GGGGS)_3$-AzF-HN / Anti-mCherry VHH-$(EAAAK)_3$-AzF-HN

COSMOGEL GST-Accept was exchanged with D-PBS(-). In a 200 μL tube, 30 μL of COSMOGEL GST-Accept was added, and after centrifugation to remove the liquid, 10 μM of GST-mCherry, GST-EmGFP,

or D-PBS(-) was added in a volume of 30 μL and incubated at room temperature at 800 rpm for 30 min. The supernatant was removed by centrifugation, and the pellet was resuspended in 30 μL of 10 μM VHH, VHH-$(GGGGS)_3$, or VHH-$(EAAAK)_3$, followed by further incubation at 4 °C at 500 rpm for 30 min. Using Ultrafree -MC (HV, 0.45 μm), the resin was removed by centrifugation at 12000 × g for 1 min (Flowthrough fraction), and then washed by adding 30 μL D-PBS(-) and centrifuging again at 12000 × g. The resin was then treated with 30 μL of 100 mM glutathione solution and centrifuged at 12000 × g for 1 min (Elution fraction). DBCO-PEG_4-5/6-FAM was added to each fraction, incubated at 37 °C for 30 min, and then subjected to SDS-PAGE for imaging of FAM-derived fluorescence and CBB staining.

Transfection of tANCHOR-mCherry Expression Plasmid and Generation of Stable Cell Lines

The tANCHOR [62] provides a versatile tool for displaying mCherry on the outer membrane. The plasmid was subsequently cloned into the Piggy Bac Transposon vector system PB533A-2 (G418 resistant). HeLa cells were seeded at 1.0×10^4 cells/well in a 96-well plate and transfected at 80% confluency. For each well, 0.6 μL of FuGENE 6 and 0.1 μg of the *tANCHOR*-mCherry plasmid, along with transposase vector, were mixed in a total volume of 5 μL with Opti-MEM Reduced Serum Medium and added to the medium. 48 h post-transfection, selection for the resistance gene was performed in DMEM (10% FBS, 1% penicillin-streptomycin-glutamine (PSG)) containing 0.8 mg/mL of antibiotic G418. Five days after the non-transfected HeLa cells died, colony isolation was conducted by the limiting dilution method, and cells were seeded at one cell per well in a 96-well plate. The medium was exchanged every other day until cells reached 80% confluence, followed by scaling up to 48-well, 24-well, 12-well, and 6-well plates. The fluorescence of mCherry was observed using an OLYMPUS IX73 microscope.

Detection of Membrane Surface mCherry in Stable Cell Lines

HeLa cells were seeded at 2.0×10^4 cells/well in a 96-well plate and cultured for 24 h. The cells were then fixed with 4% paraformaldehyde at 15 °C for 10 min and washed twice with 300 mL of D-PBS(-). The cells were blocked for 2 h with 200 μL of blocking buffer (D-PBS(-) containing 3% bovine serum albumin). Subsequently, 100 μL of diluted primary antibodies (anti-mCherry-Rabbit IgG (1 mg/mL), anti-FLAG-Rabbit IgG (1 mg/mL) in blocking buffer were added and incubated for 2 h. The cells were then washed three times with 300 μL of 0.05% D-PBS(-) with Tween. This was followed by a 2-hour incubation with 100 μL of diluted secondary antibody (anti-Rabbit IgG-HRP (0.1 mg/mL)) in blocking buffer. The cells were washed five times with 300 μL of 0.05% Tween-20 in D-PBS(-)(v/v). Each well was then incubated with 100 μL of TMB (3,3′,5,5′-tetramethylbenzidine) substrate at room temperature for 30 min, followed by the addition of 100 μL of stop solution (2 M HCl). The absorbance at 450 nm

for each well was measured using a Varioskan microplate reader.

Introduction of Alkyne Groups onto the Surface of GFP-HeLa Cells via Metabolic Labeling

GFP-HeLa were incubated in DMEM (10% FBS, 1% PSG) for 24 h, after which the medium was replaced with DMEM (10% FBS, 1% PSG) containing 40 μM N-(4-pentynoyl)-mannosamine-tetraacylated (Ac_4ManNAlk) and further incubated for 48 h. The control group was incubated in DMEM (10% FBS, 1% PSG) with 0.1% DMSO. The medium was then exchanged with DMEM containing 50 μM $CuSO_4$, 300 μM 2-(4-((Bis-((1-(tert-butyl)-1H-1,2,3-triazol-4-yl)methyl)amino)methyl)-1H-1,2,3-triazol-1-yl)acetic acid (BTTAA), 2500 μM ascorbic acid, and 50 μM 5/6-Texas Red-PEG_3-Azide. And the cells were reacted at 4 °C for 5 min. The fluorescence of Texas Red was observed using an OLYMPUS IX73 microscope.

Conjugation of Alkyne-Introduced GFP-HeLa Cells with Various VHHs

GFP-HeLa cells, previously modified to present alkyne groups, were detached using an equal-volume mixture of Accutase and 0.25% trypsin. Subsequently, each variant of VHH (VHH, VHH-$(GGGGS)_3$, and VHH-$(EAAAK)_3$) was fluorescently labeled with Alexa Fluor 647 NHS ester to determine the degree of labeling. To determine and achieve a uniform labeling density of each VHH variant on the cell surface, the cells were resuspended in 200 μL of D-PBS(-). This suspension contained 1% BSA, 50 μM $CuSO_4$, 300 μM BTTAA, 2.5 mM ascorbic acid, and varying concentrations of VHHs (40 μM and 70 μM for VHH-$(GGGGS)_3$, 40 μM and 70 μM for VHH-$(EAAAK)_3$, and 40 μM and 100 μM for VHH), with a cell density adjusted to 7.5×10^4 cells per sample. After incubating for 120 min at 4 °C, the cell suspension was filtered through a 40 μm cell strainer. Subsequently, the modification density of each VHH variant at various concentrations was quantified using a Gallios Flow Cytometer (Beckman Coulter).

Cell-cell interaction between mCherry-coated cells and various VHH-cell conjugates

After achieving a uniform labeling density of each VHH variant on the cell surface (40 μM for VHH-$(GGGGS)_3$, 70 μM for VHH-$(EAAAK)_3$, and 100 μM for VHH), mCherry stable cell lines were seeded at a density of 5×10^5 cells/well in a 4-well chamber and incubated for 24 h. Subsequently, the suspension of each VHH-modified cells was added. The cells were then incubated at 37 °C in a 5% CO_2 environment. After 30 min, 400 μL of Hank's Balanced Salt Solution with 10% FBS was added, and the cells were washed for 5 min at 1000 rpm using an Eppendorf ThermoMixer C.

2.3 Results

2.3.1 Evaluation of azide reactivity in various anti-mCherry VHHs

The reactivity of azide groups in VHH, VHH-$(GGGGS)_3$, and VHH-$(EAAAK)_3$, obtained through purification using an HN tag, was evaluated. Groups treated with DBCO-PEG_4-5/6-FAM and groups without treatment were analyzed by SDS-PAGE. In the gel stained with CBB, bands were observed at a molecular mass of approximately 16 kDa (Fig. 1a). Furthermore, when the gel was imaged for fluorescence, the groups treated with DBCO-FAM showed fluorescence signals at the same positions as the respective VHHs observed in the CBB staining (Fig. 1b). These results indicate that each VHH retains reactive azide groups.

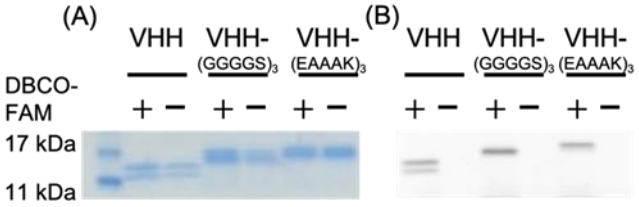

Fig. 1. Reactivity of azide groups in various anti-mCherry VHHs

Three types of VHHs (VHH, VHH-$(GGGGS)_3$, or VHH-$(EAAAK)_3$) were expressed and purified using *Escherichia coli* and subsequently reacted with DBCO-FAM. The analysis was conducted via SDS-PAGE. The image displays the gel after CBB staining (a) and the fluorescence imaging of the gel before CBB staining (b). Fluorescence images were taken with ImageQuant LAS 4000. Exposure time = 2 ms

2.3.2 Establishment of mCherry-coated HeLa cell line

HeLa cell line expressing mCherry on the cell membrane was established using the *tANCHOR* system. The intracellular expression of the FLAG tag and the membrane expression of mCherry was utilized to evaluate the cell line with a cell-based assay, using anti-FLAG and anti-mCherry antibodies as primary antibodies, and anti-Rabbit IgG (HRP conjugate) as the secondary antibody (Fig. 2). The cells treated with anti-mCherry antibody showed the highest activity, and significantly higher HRP activity was observed compared to cells treated with anti-FLAG antibody. These results suggest that mCherry is expressed extracellularly.

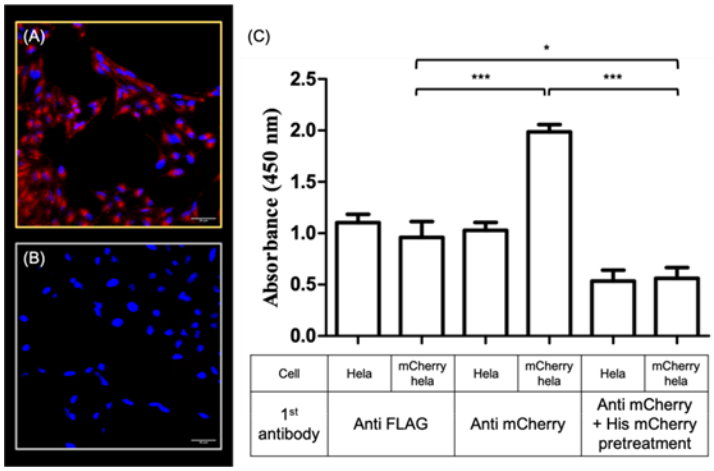

Fig. 2. Establishment and analysis of mCherry-coated HeLa cell line using tANCHOR

A HeLa cell line expressing mCherry on the cell membrane was successfully established utilizing the tANCHOR system. Fluorescence microscopy images of the mCherry-coated HeLa cells (a) and regular HeLa cells (b) were captured (OLYMPUS IX73) and showed Texas Red (red) and DAPI (blue) staining. Scale bar = 100 μm. (c) Both cell types were seeded and cultured for 24 h, followed by fixation with 2% formaldehyde. Primary antibodies targeting either Flag tags or mCherry were added to the cells, then reacted with HRP-conjugated secondary antibodies. Subsequently, HRP activity was measured at an absorbance of 450 nm. As a control, a group where the primary antibody against mCherry was reacted with an excess amount of mCherry was prepared. Each result represents the mean ± S.D and is performed in Tukey's test. *** $p < 0.001$, * $p < 0.05$.

2.3.3 Evaluation of antigen binding ability of each anti-mCherry VHH

Solutions containing GST-tagged mCherry or EmGFP, as well as solutions without these proteins, were added to glutathione agarose resin. After removing unbound GST-tagged mCherry or EmGFP, solutions containing VHH, VHH-$(GGGGS)_3$, and VHH-$(EAAAK)_3$ were added. The unbound VHH solutions (Flowthrough fraction) and the solutions obtained after washing with D-PBS(-) and adding 100 mM glutathione solution (Elution fraction) were analyzed by SDS-PAGE (Fig. 3). In this evaluation if each VHH binds to the antigen mCherry, both the mCherry on the resin and the VHH bound to mCherry would elute together in the Elution fraction. For all VHHs, bands corresponding to VHH were observed at approximately 15 to 18 kDa in the Elution fraction of the resin bound to mCherry. This indicates that all VHHs have the ability to bind to mCherry. Furthermore, in the case of resin with no binding or resin bound to EmGFP, VHH bands were observed in the Flowthrough fraction, but not in the Elution fraction. This demonstrates that all VHHs specifically bind to the antigen mCherry.

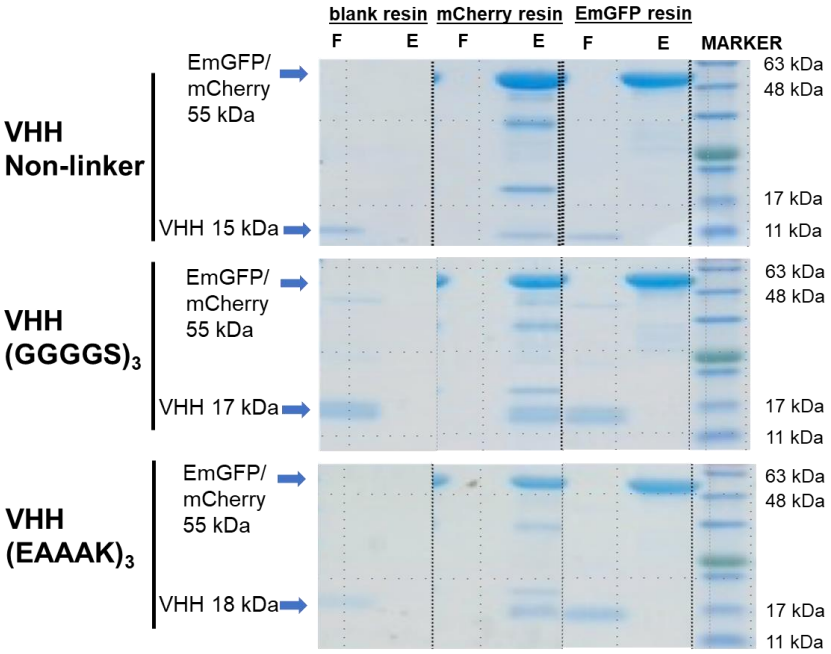

Fig. 3. Antigen binding capacity of various anti-mCherry VHHs

After binding mCherry or EmGFP to the resin via a GST-tag, three types of VHH (VHH, VHH-$(GGGGS)_3$, or VHH-$(EAAAK)_3$) were added. The unbound fractions (F=Flowthrough) and the bound fractions obtained by the addition of 100 mM glutathione (E=Elution) were analyzed by SDS-PAGE, respectively, and the gels were stained with CBB

2.3.4 Introduction of alkyne groups to the surface of HeLa cells using metabolic labeling

The introduction of alkyne groups on the cell membrane surface of HeLa cells was investigated using 5/6-Texas Red-PEG_3-Azide. This was done in HeLa cells treated with Ac_4ManNAlk. as well as in untreated HeLa cells. Fluorescence signals were observed in HeLa cells treated with Ac4ManNAlk (Fig. 4a), but no signals were detected in untreated HeLa cells (Fig. 4b). These results demonstrate that alkyne groups were successfully introduced into HeLa cells via Ac_4ManNAlk treatment.

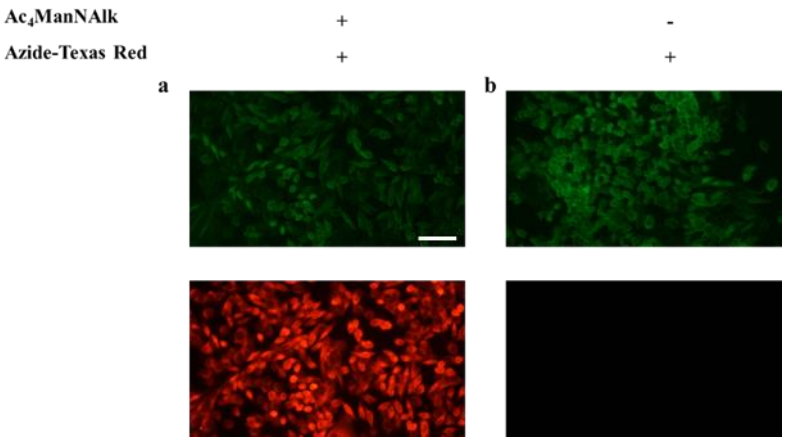

Fig. 4. Confirmation of GFP HeLa cells labeling with Alkyne

GFP-HeLa cells were cultured for 48 h in DMEM medium containing 40 μM Ac_4ManNAlk (a) or DMEM medium with 0.1% DMSO (b). Subsequently, the cells were incubated in DMEM medium containing 50 μM 5/6-Texas Red-PEG_3-Azide, 50 μM $CuSO_4$, 300 μM BTTAA, and 2500 μM ascorbic acid at 4 °C for 5 min. The cells were observed under a fluorescence microscope (Olympus IX73) with an FITC (upper) or TRITC (lower) filter. Scale bar = 100 μm

2.3.5 Enhancement of cell adhesion to mCherry-coated HeLa cells via VHH modification and peptide spacers

In order to assess the impact of anti-mCherry VHH modification on cell adhesion, GFP-HeLa cells, either modified with various VHH through spacers or unmodified, were added to mCherry-coated HeLa cells seeded on a dish. Additionally, each VHH modification density on GFP HeLa cells was similar (Fig. 5a). It revealed that the VHH-modified GFP-HeLa cells exhibited a significantly higher adhesion to the mCherry-coated HeLa cells, as compared to their unmodified counterparts (Fig. 5b). Notably, the incorporation of peptide spacers between the VHH and GFP-HeLa cells further augmented this adhesion effect. These findings underscore the effectiveness of VHH modification, particularly when coupled with peptide spacers, in enhancing cellular adhesion to target cells expressing specific antigens.

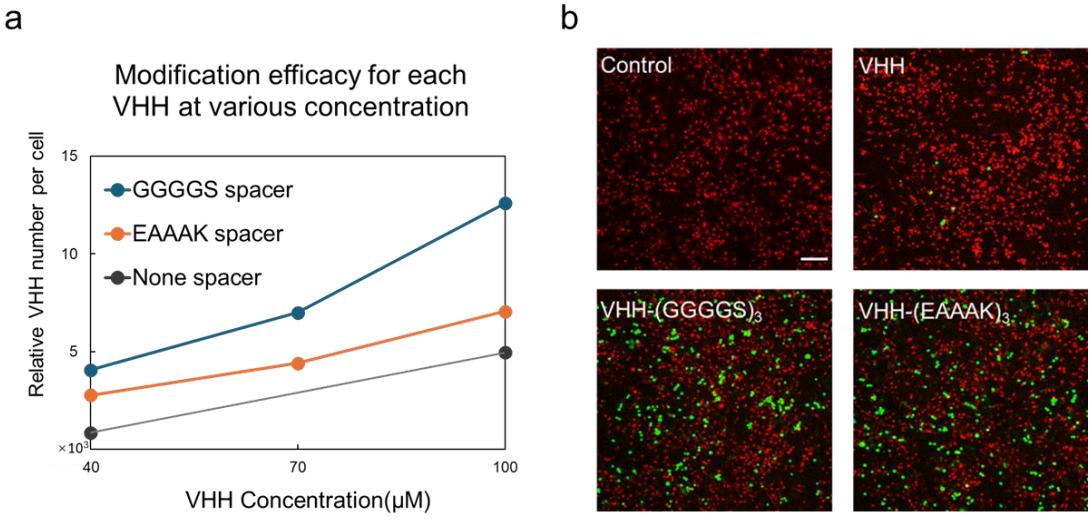

Fig. 5. Enhancement of adhesion to mCherry-coated HeLa cells

a) To achieve a similar modification density across each VHH variant, specific concentrations were selected: 40 μM for VHH-$(GGGGS)_3$, 70 μM for VHH-$(EAAAK)_3$, and 100 μM for VHH. These concentrations were chosen based on the relative VHH number per cell at various concentrations. b) After seeding and culturing mCherry-coated HeLa cells for 24 h, suspensions of GFP-HeLa cells modified with various VHH or unmodified GFP-HeLa cells (control) were added and incubated for 30

min at 37 °C in 5% CO_2. Following the removal of unadhered GFP-HeLa cells, the samples were fixed with 4% paraformaldehyde and observed using a confocal laser microscope system. Scale bar = 100 μm

2.4 Discussion

My data demonstrates a notable enhancement in cell-cell interaction facilitated by the incorporation of specific spacers in the form of GS and EK spacers within VHH-cell conjugates. In contrast, groups lacking these spacers did not exhibit similar interaction capacities. This observation aligns with the understanding that in HeLa-VHH conjugation, the HeLa cell surface is enveloped by a glycocalyx layer approximately 20 nm thick [86]. The significance of this dimension becomes evident when considering the T cell binding model, where crystal structures of a TCR–MHC complex, spanning nearly 15 nm, must traverse the glycocalyx barrier to make effective contact [87]. Given that the size of an anti-mCherry VHH is around 4 nm [60], its direct conjugation to glycoproteins [54] may be insufficient for antigen binding due to the dimensional constraints imposed by the glycocalyx. However, extending the VHH with either a $(GGGGS)_3$ spacer (approximately 5.8 nm [88]) or an $(EAAAK)_3$ spacer (approximately 7 nm [89]) provides the necessary spatial allowance for effective binding. The work of D. Moritz et al. further corroborates the importance of spacers in cellular interactions [83]. They observed that only CAR-T cells incorporating a spacer region exhibited ErbB-2 binding activity in T cells, while constructs lacking a spacer segment did not. Moreover, softer spacers are purported to be more effective in cell-cell interactions than rigid ones. Zhang et al. [85] reported decreased cytokine release and lower cell-cell interaction in CAR-T cells with mutated amino acids in the spacer domain, reducing its flexibility while maintaining CAR expression levels. Similarly, Wilkie et al. [90] found that MUC-1 CAR-T cells with a flexible IgD spacer released higher levels of interferon and showed enhanced cellular interactions compared to those with a rigid IgG1 spacer, despite lower CAR expression in the former. However, my results reveal that both soft and tough spacers exhibit similar levels of cell-cell interaction. This outcome suggests that due to the conjugation of VHH to glycoproteins, the substantial size of the glycocalyx overshadows the contribution of the spacer's size, and flexibility is primarily governed by the glycocalyx itself. As a result, both glycocalyx-VHH-$(GGGGS)_3$ and glycocalyx-VHH-$(EAAAK)_3$ configurations might exhibit comparable levels of flexibility, leading to a similar extent of cell-cell interaction.

In my study, to achieve a comparable level of cell-surface modification across different VHH variants, I observed that a concentration of 40 μM for VHH with a $(GGGGS)_3$ spacer was equivalent to 70 μM for those with an $(EAAAK)_3$ spacer and 100 μM for non-spacer VHHs. This finding suggests that the inclusion of a spacer not only enhances the efficiency of cell-VHH conjugation but also indicates that a

softer spacer may be more effective than a stiffer one. The importance of a flexible spacer in these conjugations cannot be overstated. Flexible spacers provide spatial freedom and reduce steric hindrance, thereby leading to higher reaction yields. This observation is supported by Andre's study [91], where the coupling of trypsin to magnetic nanoparticles using a spacer composed of 12 PEG groups resulted in a 30% increase in reaction yield compared to a configuration without a spacer. Similarly, Salaun's investigation [92] demonstrated that the incorporation of a flexible $(GGGGS)_2$ spacer or a rigid $(AP)_6$ spacer between the acylation domain and the main body of SNAP25 (synaptosome-associated protein of 25 kDa) led to a two-fold increase in acylation yield. Notably, the flexible spacer outperformed the rigid one, further emphasizing the benefits of flexibility in such molecular configurations. These findings collectively underscore the significance of flexible spacers in enhancing the yield of cell-antibody conjugations. By providing the necessary spatial accommodation and minimizing steric clashes, flexible spacers facilitate more efficient and effective conjugation processes, which can be crucial in the development and optimization of cell-based therapeutic strategies.

When considering the application of these findings to other proteins and cell types, it becomes crucial to reevaluate the choice of peptide spacer. The length of the spacer is particularly important, as the distance of receptors from the cell surface can vary considerably among different cell types. For example, CD28 extends approximately 7.5 nm from the cell surface, while CD45 reaches nearly 40 nm [93]. Therefore, the length of the spacer, such as the $(GGGGS)_n$, should be carefully optimized by adjusting the copy number “n” to achieve the desired cell-cell interaction. In addition to the length, the production and proper folding of the target protein can sometimes be challenging when fused with a GGGGS spacer. In such instances, alternative flexible spacers may need to be considered to enhance protein folding and expression. For instance, a $(Gly)_8$ spacer has been shown to facilitate the expression of Myc-Est2p in yeast [94], while a $(Gly)_6$ spacer has been effective in ensuring the correct folding and maintenance of bioactivity in Albumin-ANF fusion proteins [86]. These examples highlight the importance of carefully selecting and potentially customizing the spacer not only for effective cell-cell interaction but also for optimal protein production and functionality.

Summary

Chemical molecules exhibit remarkable reaction selectivity and robust covalent bond formation, making them potentially valuable for achieving programmed immobilization of living cells through chemical reactions. However, many chemical reactions are unsuitable for living cells due to their inability to react effectively within a cellular environment. Nevertheless, click chemistry pairs stand out as highly bio-compatible and bio-orthogonal. To exploit this, I introduced click chemistry substrates onto cell membranes and cover glasses, with the goal of programmed anchoring living cells onto the glass via covalent bonds. Initially, Azide-group labeled living cells were prepared by metabolic labeling with Ac_4ManNAz for 48 h. Following the introduction of Az, TCO was metabolically labeled into the living cells by reacting with TCO-PEG_{12}-DBCO. Az and TCO in the cells were detected using DBCO-FAM and Tetrazine-Cy3, respectively. The cover glasses were cleansed using piranha solution, followed by a silanization process to attach thiol ligands. Subsequently, they were treated with maleimide-PEG-amino or maleimide-PEG-methyl to add amino or methyl groups. Lastly, the glasses with amino groups were further modified with DBCO or Tetrazine molecules through reactions with DBCO-COOH or Tetrazine-PEG_5-NHS, respectively. The mixture of Az-labeled green fluorescent protein HeLa cells and TCO-labeled red fluorescent protein HeLa cells was reacted in a culture dish in which three different cover glasses, DBCO-, Tetrazine-, or methyl-coated, were added. Az- or TCO-labeled cells could be immobilized in a functional group-dependent manner.

Aligned antibody immobilization leads to effective antigen recognition. Site incorporating Azido-phenylalanine into antibody is helpful to achieve site-specific conjugation, which reveals aligned antibody immobilization. Initially, azido-phenylalanine was introduced to fluorescent protein mKO2. The mKO2-Az was immobilized on the DBCO-coated glass within 30 min of reaction, while mKO2 without Az modification remained unbound. These findings demonstrate that DBCO on the substrate enables immobilization of AzF tagged proteins. Anti-mCherry VHH and anti-EmGFP VHH, with AzF introduced at the C-terminus, distal to its antigen-binding site for the mCherry and EmGFP, were expressed and purified in *Escherichia coli*. Through a GST-tag, mCherry was bound to resin, and VHH was then added. The bound and unbound fractions obtained after the addition of glutathione were analyzed using SDS-PAGE. Bands for both mCherry and VHH were observed in the bound fraction but not in the unbound fraction, confirming the binding of VHH to mCherry. And Anti-EmGFP VHH yields similar results. Following the conjugation of both VHH-Az to the DBCO substrate, a mixture of mCherry and EmGFP proteins was applied to the surface. Each protein selectively adhered to its complementary VHH. Finally, HeLa cells expressing mCherry on their surfaces (mCherry-coated cells) were incubated with an anti-mCherry VHH-coated substrate for 1 h. This resulted in increased immobilization of mCherry-coated cells on the VHH substrate, while normal HeLa cells did not adhere.

In the pursuit of establishing cell-cell interaction, introducing aligned low molecular mass antibodies (VHH) into the cell membrane to enhance intercellular adhesion with specific cells proves beneficial for programmed cell-cell stacking. In particular, analogous to the spacer section that augments antigen recognition in chimeric antigen receptor T cells, I believed it was helpful to improve cell-cell stacking by incorporating peptide spacers between VHH and cells. Initially, Anti-mCherry VHH with Az was prepared for the selective cell adhesion. After introducing the alkyne group on GFP-HeLa cells, VHH connected GFP-cells via click reaction. I proceeded to generate VHH constructs incorporating two distinct peptide spacers between VHH and Az: a flexible three-repeat of glycine- glycine-glycine-glycine-serine (GGGGS) and a more rigid three-repeat of glutamic acid-alanine-alanine-alanine-lysine (EAAAK). I harvested mCherry coated cells on plates as the first cell layer. VHH conjugated or unmodified GFP-cells were incubated over the first cell layer, mCherry-coated cells. More VHH-cells remained on the first cell layer than unmodified cells. And both peptide spacers enhanced the cell adhesion on the first cell layer compared with non-spacer VHH. VHH with peptide linker is helpful for programmed cell immobilization to the target cells.

In conclusion, I successfully employed independent click pairs and interaction of antigen-aligned -VHH-antibodies to selectively manage cell adhesion, achieving patterned cell organization on various surfaces and layers.

Reference

1 Mazaafrianto, D. N., Maeki, M., Ishida, A., Tani, H. & Tokeshi, M. Recent microdevice-based aptamer sensors. *Micromachines* **9**, 202 (2018).

2 Gupta, N., Renugopalakrishnan, V., Liepmann, D., Paulmurugan, R. & Malhotra, B. D. Cell-based biosensors: Recent trends, challenges and future perspectives. *Biosensors and Bioelectronics* **141**, 111435 (2019).

3 Chai, C. & Leong, K. W. Biomaterials approach to expand and direct differentiation of stem cells. *Molecular therapy* **15**, 467-480 (2007).

4 Edmondson, R., Broglie, J. J., Adcock, A. F. & Yang, L. Three-dimensional cell culture systems and their applications in drug discovery and cell-based biosensors. *Assay and drug development technologies* **12**, 207-218 (2014).

5 Khademhosseini, A., Langer, R., Borenstein, J. & Vacanti, J. P. Microscale *technologies for tissue engineering and biology. Proceedings of the National Academy of Sciences* **103**, 2480-2487 (2006).

6 Thomsen, T. & Klok, H.-A. Chemical cell surface modification and analysis of nanoparticle-modified living cells. *ACS applied bio materials* **4**, 2293-2306 (2021).

7 Saxon, E. & Bertozzi, C. R. Cell surface engineering by a modified Staudinger reaction. *Science* **287**, 2007-2010 (2000).

8 Teramura, Y. & Iwata, H. Cell surface modification with polymers for biomedical studies. *Soft Matter* **6**, 1081-1091 (2010).

9 Scheideler, O. J. *et al.* Recapitulating complex biological signaling environments using a multiplexed, DNA-patterning approach. *Science advances* **6**, eaay5696 (2020).

10 Todhunter, M. E. *et al.* Programmed synthesis of three-dimensional tissues. *Nature methods* **12**, 975-981 (2015).

11 Vermesh, U. *et al.* High-density, multiplexed patterning of cells at single-cell resolution for tissue engineering and other applications. *Angewandte Chemie (International ed. in English)* **50**, 7378 (2011).

12 Twite, A. A., Hsiao, S. C., Onoe, H., Mathies, R. A. & Francis, M. B. Direct attachment of microbial organisms to material surfaces through sequence-specific DNA hybridization. *Advanced Materials (Deerfield Beach, Fla.)* **24**, 2380-2385 (2012).

13 Hsiao, S. C. *et al.* Direct cell surface modification with DNA for the capture of primary cells and the investigation of myotube formation on defined patterns. *Langmuir* **25**, 6985-6991 (2009).

14 Mbua, N. E., Guo, J., Wolfert, M. A., Steet, R. & Boons, G. J. Strain-promoted alkyne–azide cycloadditions (SPAAC) reveal new features of glycoconjugate biosynthesis. *ChemBioChem* **12**, 1912-1921 (2011).

15 Agard, N. J., Prescher, J. A. & Bertozzi, C. R. A strain-promoted [3+ 2] azide− alkyne cycloaddition for covalent modification of biomolecules in living systems. *Journal of the American Chemical Society* **126**, 15046-15047 (2004).

16 Blackman, M. L., Royzen, M. & Fox, J. M. Tetrazine ligation: fast bioconjugation based on inverse-electron-demand Diels− Alder reactivity. *Journal of the American Chemical Society* **130**, 13518-13519 (2008).

17 Prescher, J. A. & Bertozzi, C. R. Chemistry in living systems. *Nature chemical biology* **1**, 13-21 (2005).

18 Prescher, J. A., Dube, D. H. & Bertozzi, C. R. Chemical remodelling of cell surfaces in living animals. *Nature* **430**, 873-877 (2004).

19 Karver, M. R., Weissleder, R. & Hilderbrand, S. A. Bioorthogonal reaction pairs enable simultaneous, selective, multi-target imaging. *Angewandte Chemie* **124**, 944-946 (2012).

20 Hahn, J., Wickham, S. F., Shih, W. M. & Perrault, S. D. Addressing the instability of DNA nanostructures in tissue culture. *ACS nano* **8**, 8765-8775 (2014).
21 Chalaya, T., Gogvadze, E., Buzdin, A., Kovalskaya, E. & Sverdlov, E. D. Improving specificity of DNA hybridization-based methods. *Nucleic acids research* **32**, e130-e130 (2004).
22 Paludan, S. R. Activation and regulation of DNA-driven immune responses. *Microbiology and Molecular Biology Reviews* **79**, 225-241 (2015).
23 Hong, V., Steinmetz, N. F., Manchester, M. & Finn, M. Labeling live cells by copper-catalyzed alkyne− azide click chemistry. *Bioconjugate chemistry* **21**, 1912-1916 (2010).
24 Haga, Y. *et al.* Visualizing specific protein glycoforms by transmembrane fluorescence resonance energy transfer. *Nature communications* **3**, 907 (2012).
25 Yuan, Y., Xu, S., Cheng, X., Cai, X. & Liu, B. Bioorthogonal turn-on probe based on aggregation-induced emission characteristics for cancer cell imaging and ablation. *Angewandte Chemie International Edition* **55**, 6457-6461 (2016).
26 Han, S.-S. *et al.* Physiological effects of Ac4ManNAz and optimization of metabolic labeling for cell tracking. *Theranostics* **7**, 1164 (2017).
27 Champion, L., Linder, M. I. & Kutay, U. Cellular reorganization during mitotic entry. *Trends in cell biology* **27**, 26-41 (2017).
28 Martin, K. H., Slack, J. K., Boerner, S. A., Martin, C. C. & Parsons, J. T. Integrin connections map: to infinity and beyond. *Science* **296**, 1652-1653 (2002).
29 Hynes, R. O. Integrins: versatility, modulation, and signaling in cell adhesion. *Cell* **69**, 11-25 (1992).
30 Wada, T. *et al.* Cloning, expression, and chromosomal mapping of a human ganglioside sialidase. *Biochemical and biophysical research communications* **261**, 21-27 (1999).
31 Howlader, M. A., Guo, T., Chakraberty, R. & Cairo, C. W. Isoenzyme-selective inhibitors of human neuraminidases reveal distinct effects on cell migration. *ACS Chemical Biology* **15**, 1328-1339 (2020).
32 Jia, F., Howlader, M. A. & Cairo, C. W. Integrin-mediated cell migration is blocked by inhibitors of human neuraminidase. *Biochimica et Biophysica Acta (BBA)-Molecular and Cell Biology of Lipids* **1861**, 1170-1179 (2016).
33 Debets, M. F. *et al.* Metabolic precision labeling enables selective probing of O-linked N-acetylgalactosamine glycosylation. *Proceedings of the National Academy of Sciences* **117**, 25293-25301 (2020).
34 Cohen, A. S., Dubikovskaya, E. A., Rush, J. S. & Bertozzi, C. R. Real-time bioluminescence imaging of glycans on live cells. *Journal of the American Chemical Society* **132**, 8563-8565 (2010).
35 Mahal, L. K., Yarema, K. J. & Bertozzi, C. R. Engineering chemical reactivity on cell surfaces through oligosaccharide biosynthesis. *Science* **276**, 1125-1128 (1997).
36 Song, K. H., Highley, C. B., Rouff, A. & Burdick, J. A. Complex 3D-printed microchannels within cell-degradable hydrogels. *Advanced Functional Materials* **28**, 1801331 (2018).
37 Kulkarni, P., Parkale, R., Khare, S., Kumar, P. & Arya, N. Cell immobilization strategies for tissue engineering: Recent trends and future perspectives. *Immobilization Strategies: Biomedical, Bioengineering and Environmental Applications*, 85-139 (2021).
38 Gui, Q., Lawson, T., Shan, S., Yan, L. & Liu, Y. The application of whole cell-based biosensors for use in environmental analysis and in medical diagnostics. *Sensors* **17**, 1623 (2017).
39 Michelini, E. & Roda, A. Staying alive: new perspectives on cell immobilization for biosensing purposes. *Analytical and bioanalytical chemistry* **402**, 1785-1797 (2012).
40 Melamed, S. *et al.* A printed nanolitre-scale bacterial sensor array. *Lab on a Chip* **11**, 139-146 (2011).

41 Selimoglu, S. M. & Elibol, M. Alginate as an immobilization material for MAb production via encapsulated hybridoma cells. *Critical reviews in biotechnology* **30**, 145-159 (2010).
42 Yamashita, T. *et al.* A novel open-type biosensor for the in-situ monitoring of biochemical oxygen demand in an aerobic environment. *Scientific reports* **6**, 38552 (2016).
43 Suo, Z. *et al.* Antibody selection for immobilizing living bacteria. *Analytical chemistry* **81**, 7571-7578 (2009).
44 Kawamura, R. *et al.* A new cell separation method based on antibody-immobilized nanoneedle arrays for the detection of intracellular markers. *Nano Letters* **17**, 7117-7124 (2017).
45 Rabe, M., Verdes, D. & Seeger, S. Understanding protein adsorption phenomena at solid surfaces. *Advances in colloid and interface science* **162**, 87-106 (2011).
46 Vashist, S. K., Lam, E., Hrapovic, S., Male, K. B. & Luong, J. H. Immobilization of antibodies and enzymes on 3-aminopropyltriethoxysilane-functionalized bioanalytical platforms for biosensors and diagnostics. *Chemical reviews* **114**, 11083-11130 (2014).
47 Arnau, J., Lauritzen, C., Petersen, G. E. & Pedersen, J. Current strategies for the use of affinity tags and tag removal for the purification of recombinant proteins. *Protein expression and purification* **48**, 1-13 (2006).
48 Fang, X., Tan, O. K., Gan, Y. Y. & Tse, M. S. Novel immunosensor platform based on inorganic barium strontium titanate film for human IgG detection. *Sensors and Actuators B: Chemical* **149**, 381-388 (2010).
49 Feng, B. *et al.* 3D antibody immobilization on a planar matrix surface. *Biosensors and Bioelectronics* **28**, 91-96 (2011).
50 Trilling, A. K., Beekwilder, J. & Zuilhof, H. Antibody orientation on biosensor surfaces: a minireview. *Analyst* **138**, 1619-1627 (2013).
51 Kang, J. H. *et al.* Improving immunobinding using oriented immobilization of an oxidized antibody. *Journal of Chromatography a* **1161**, 9-14 (2007).
52 Baio, J., Cheng, F., Ratner, D. M., Stayton, P. S. & Castner, D. G. Probing orientation of immobilized humanized anti-lysozyme variable fragment by time-of-flight secondary-ion mass spectrometry. *Journal of Biomedical Materials Research Part A* **97**, 1-7 (2011).
53 Arbabi-Ghahroudi, M. Camelid single-domain antibodies: promises and challenges as lifesaving treatments. *International journal of molecular sciences* **23**, 5009 (2022).
54 Gartner, Z. J. & Bertozzi, C. R. Programmed assembly of 3-dimensional microtissues with defined cellular connectivity. *Proceedings of the National Academy of Sciences* **106**, 4606-4610 (2009).
55 Wang, L. & Schultz, P. G. A general approach for the generation of orthogonal tRNAs. *Chemistry & biology* **8**, 883-890 (2001).
56 Wals, K. & Ovaa, H. Unnatural amino acid incorporation in E. coli: current and future applications in the design of therapeutic proteins. *Frontiers in chemistry* **2**, 15 (2014).
57 Muyldermans, S. Nanobodies: natural single-domain antibodies. *Annual review of biochemistry* **82**, 775-797 (2013).
58 Kim, C. H., Axup, J. Y. & Schultz, P. G. Protein conjugation with genetically encoded unnatural amino acids. *Current opinion in chemical biology* **17**, 412-419 (2013).
59 Mukai, T. *et al.* Genetic-code evolution for protein synthesis with non-natural amino acids. *Biochemical and biophysical research communications* **411**, 757-761 (2011).
60 Wang, Z. *et al.* Structural insights into the binding of nanobodies LaM2 and LaM4 to the red fluorescent protein mCherry. *Protein Science* **30**, 2298-2309 (2021).
61 Kubala, M. H., Kovtun, O., Alexandrov, K. & Collins, B. M. Structural and thermodynamic analysis of the GFP: GFP-nanobody complex. *Protein Science* **19**,

2389-2401 (2010).
62 Ivanusic, D. *et al.* tANCHOR: a novel mammalian cell surface peptide display system. *Biotechniques* **70**, 21-28 (2020).
63 Trilling, A. K. *et al.* Orientation of llama antibodies strongly increases sensitivity of biosensors. *Biosensors and Bioelectronics* **65**, 130-136 (2014).
64 Balevicius, Z. *et al.* Evaluation of intact-and fragmented-antibody based immunosensors by total internal reflection ellipsometry. *Sensors and Actuators B: chemical* **160**, 555-562 (2011).
65 Chen, J., Li, Q., Li, J. & Maitz, M. F. The effect of anti-CD34 antibody orientation control on endothelial progenitor cell capturing cardiovascular devices. *Journal of Bioactive and Compatible Polymers* **31**, 583-599 (2016).
66 Trilling, A. K., Harmsen, M. M., Ruigrok, V. J., Zuilhof, H. & Beekwilder, J. The effect of uniform capture molecule orientation on biosensor sensitivity: Dependence on analyte properties. *Biosensors and Bioelectronics* **40**, 219-226 (2013).
67 Fischbach, M. A., Bluestone, J. A. & Lim, W. A. Cell-based therapeutics: the next pillar of medicine. *Science translational medicine* **5**, 179ps177-179ps177 (2013).
68 Goldman, S. Stem and progenitor cell–based therapy of the human central nervous system. *Nature biotechnology* **23**, 862-871 (2005).
69 Laflamme, M. A. *et al.* Cardiomyocytes derived from human embryonic stem cells in pro-survival factors enhance function of infarcted rat hearts. *Nature biotechnology* **25**, 1015-1024 (2007).
70 Barbash, I. M. *et al.* Systemic delivery of bone marrow–derived mesenchymal stem cells to the infarcted myocardium: feasibility, cell migration, and body distribution. *Circulation* **108**, 863-868 (2003).
71 Cheng, Z. *et al.* Targeted migration of mesenchymal stem cells modified with CXCR4 gene to infarcted myocardium improves cardiac performance. *Molecular Therapy* **16**, 571-579 (2008).
72 Zheng, P.-P., Kros, J. M. & Li, J. Approved CAR T cell therapies: ice bucket challenges on glaring safety risks and long-term impacts. *Drug discovery today* **23**, 1175-1182 (2018).
73 Bonifant, C. L., Jackson, H. J., Brentjens, R. J. & Curran, K. J. Toxicity and management in CAR T-cell therapy. *Molecular Therapy-Oncolytics* **3** (2016).
74 Csizmar, C. M., Petersburg, J. R. & Wagner, C. R. Programming cell-cell interactions through non-genetic membrane engineering. *Cell chemical biology* **25**, 931-940 (2018).
75 Teramura, Y., Chen, H., Kawamoto, T. & Iwata, H. Control of cell attachment through polyDNA hybridization. *Biomaterials* **31**, 2229-2235 (2010).
76 Sarkar, D. *et al.* Engineered cell homing. *Blood, The Journal of the American Society of Hematology* **118**, e184-e191 (2011).
77 Shi, P. *et al.* Spatiotemporal control of cell–cell reversible interactions using molecular engineering. *Nature communications* **7**, 13088 (2016).
78 Swee, L. K., Lourido, S., Bell, G. W., Ingram, J. R. & Ploegh, H. L. One-step enzymatic modification of the cell surface redirects cellular cytotoxicity and parasite tropism. *ACS chemical biology* **10**, 460-465 (2015).
79 Zhu, C., Takemoto, H., Higuchi, Y. & Yamashita, F. Programmed immobilization of living cells using independent click pairs. *Biochemical and Biophysical Research Communications*, 149556 (2024).
80 Rudd, A. K., Valls Cuevas, J. M. & Devaraj, N. K. SNAP-tag-reactive lipid anchors enable targeted and spatiotemporally controlled localization of proteins to phospholipid membranes. *Journal of the American Chemical Society* **137**, 4884-4887 (2015).
81 Stoiber, S. *et al.* Limitations in the design of chimeric antigen receptors for cancer therapy. *Cells* **8**, 472 (2019).
82 Larson, R. C. & Maus, M. V. Recent advances and discoveries in the mechanisms

and functions of CAR T cells. *Nature Reviews Cancer* **21**, 145-161 (2021).
83 Moritz, D. & Groner, B. A spacer region between the single chain antibody-and the CD3 zeta-chain domain of chimeric T cell receptor components is required for efficient ligand binding and signaling activity. *Gene therapy* **2**, 539-546 (1995).
84 Hudecek, M. *et al.* The nonsignaling extracellular spacer domain of chimeric antigen receptors is decisive for in vivo antitumor activity. *Cancer immunology research* **3**, 125-135 (2015).
85 Zhang, A. *et al.* Reducing hinge flexibility of CAR-T cells prolongs survival in vivo with low cytokines release. *Frontiers in Immunology* **12**, 724211 (2021).
86 Potter, D. R. & Damiano, E. R. The hydrodynamically relevant endothelial cell glycocalyx observed in vivo is absent in vitro. *Circulation research* **102**, 770-776 (2008).
87 Shaw, A. S. & Dustin, M. L. Making the T cell receptor go the distance: a topological view of T cell activation. *Immunity* **6**, 361-369 (1997).
88 Chen, X., Zaro, J. L. & Shen, W.-C. Fusion protein linkers: property, design and functionality. *Advanced drug delivery reviews* **65**, 1357-1369 (2013).
89 Ma, Q., Liu, L., Yang, Z. & Zheng, P. Facile Synthesis of Peptide-Conjugated Gold Nanoclusters with Different Lengths. *Nanomaterials* **11**, 2932 (2021).
90 Wilkie, S. *et al.* Retargeting of human T cells to tumor-associated MUC1: the evolution of a chimeric antigen receptor. *The Journal of Immunology* **180**, 4901-4909 (2008).
91 Andre, J., Saleh, D., Syldatk, C. & Hausmann, R. Effect of spacer modification on enzymatic synthetic and hydrolytic activities of immobilized trypsin. *Journal of Molecular Catalysis B: Enzymatic* **125**, 88-96 (2016).
92 Salaun, C., Greaves, J., Tomkinson, N. C. & Chamberlain, L. H. The linker domain of the SNARE protein SNAP25 acts as a flexible molecular spacer that ensures efficient S-acylation. *Journal of Biological Chemistry* **295**, 7501-7515 (2020).
93 Al-Aghbar, M. A., Jainarayanan, A. K., Dustin, M. L. & Roffler, S. R. The interplay between membrane topology and mechanical forces in regulating T cell receptor activity. *Communications Biology* **5**, 40 (2022).
94 Sabourin, M., Tuzon, C. T., Fisher, T. S. & Zakian, V. A. A flexible protein linker improves the function of epitope-tagged proteins in Saccharomyces cerevisiae. *Yeast* **24**, 39-45 (2007).

Publication list

主論文

１．題　目　Programmed cell-immobilization of living cells by independent molecular interaction
（細胞膜へのクリック反応性官能基修飾の生細胞配置固定への応用 ）

２．主論文の基礎となる学術論文の公表の方法・時期

第１章　題　目　Programmed immobilization of living cells modified with click reactive functional groups
（クリック反応性官能基を修飾した生細胞の配置固定）

Chengyuan Zhu, Hiroyasu Takemoto, Yuriko Higuchi*, and Fumiyoshi Yamashita. Programmed immobilization of living cells using independent click pairs.″ *Biochemical and Biophysical Research Communications* (2024): 149556.

第２章　題　目　Programmed immobilization of living cells via antigen - VHH antibody interaction
(VHH 抗体と抗原の相互作用を利用した生細胞の配置固定)

未発表

第２章　題　目　Effect of peptide spacer between VHH antibody and cell membrane on programmed immobilization of living cells
(生細胞の配置固定における VHH 抗体と細胞膜の間のペプチドスペーサーの影響)

未発表

Acknowledgement

I extend my deepest gratitude to Professor Yuriko Higuchi, my dissertation advisor, for her unwavering support and invaluable guidance throughout this academic journey. Her expertise and insightful feedback have been instrumental in shaping both the substance of this dissertation and my development as a Ph.D. candidate.

My sincere appreciation goes to the members of my dissertation committee. Their thoughtful critiques and encouragement have significantly enriched my research, providing diverse perspectives and insightful suggestions that have been integral to my work.

I am profoundly thankful to my colleagues and peers in the Department of Drug Delivery Research. The spirit of teamwork and shared knowledge within our department has been a constant source of inspiration and motivation. Special acknowledgment is due to Mr. Yuta Ichikawa and Mr. Kazunori Tomita, whose consistent support and constructive discussions have been invaluable to my research.

I am also deeply grateful to Professor Hiroyasu Takemoto of Kyoto Prefectural University of Medicine for his general support, which made this research possible. My sincere gratitude extends to Professor Hiroyasu Takemoto of RIKEN for generously providing pCDF/pAzAz and facilitating our work on VHH-AzF proteins.

To my friends and family, I owe heartfelt thanks for their endless love, patience, and understanding. Their unwavering belief in me has been a pillar of strength and a source of constant encouragement.

I am thankful to all the participants and individuals who contributed to this study. Their involvement has been critical in bringing this research to fruition.

This dissertation is a testament to the collaborative efforts and kindness of all those mentioned, and many unmentioned, who have accompanied me on this academic voyage.